PROJECT SEMESTER REPORT

(Project Semester Jan-June 2018)

DYNAMIC ANALYSIS OF ROBOTIC MANIPULATOR

Submitted by:

SHASHWAT JAIN

(101508113)

Under the Guidance of:

Faculty Mentor

Dr. ANU MITTAL

(Assistant Professor)

Research Guide

Dr. SANJEEV SONI

(Senior Scientist)

DEPARTMENT OF MECHANICAL ENGINEERING

THAPAR INSTITUTE OF ENGINEERING & TECHNOLOGY, PATIALA

(Declared as Deemed-to-be-University u/s 3 of the UGC Act, 1956)

July 2018

DECLARATION

I hereby declare that the project work entitled "Dynamic analysis of robotic manipulator", is an authentic record of my own work carried out at Biomedical instrumentation department, CSIR-CSIO, Chandigarh as requirements of six months project semester for the award of degree of B.E. (Mechanical), Thapar Institute of Engineering and Technology, Patiala under the guidance of Dr. Sanjeev Soni (Senior scientist) and Dr. Anu Mittal (Assistant Professor), during January to June, 2018.

Shashwat Jain
101508113

Date: 8 Aug 2018

Certified that the above statement made by the student is correct to the best of our knowledge and belief.

Dr. Sanjeev Soni
Senior Scientist
Biomedical instrumentation department
CSIR-CSIO, Chandigarh

Dr. Anu Mittal
Assistant Professor
Mechanical Engineering Department,
Thapar Institute of Engineering and Technology

Abstract

Nowadays, robotic manipulators are extensively used in various applications like surgery, welding, assembling, laser cutting, etc. There is a need to simulate these systems to get things done quickly and efficiently to keep cost down and projects on time. With simulations, real life phenomena, processes and systems can be replicated, fine tuned and predicted on computers.

In recent times applications of robotics have emerged beyond the field of manufacturing and they are now widely used in medical sector also. One important use of robots is in surgery where surgical robots carry out operations with great precision than an unaided human surgeon. These robotic manipulators have a certain dynamics and behavior depending on the components and their geometry as well as external forces and motions applied to them. So, there is a need of a simulation tool to solve these multi-body problems and for this project we have chosen MSC Software Corporation's ADAMS due to its familiarity and features. Our purpose of this project is to perform the dynamic analysis of robotic manipulator in ADAMS software and selecting the appropriate motors for the movement of robot joints and study the joint torque characteristics. Also appropriate friction model is incorporated to calculate the value of joint friction.

Contents

List of figures

Chapter 1

Introduction

Robotics is concerned with the study of complex machines that can replace human beings and can perform task better than humans in some ways. The goal of this introductory chapter is to give overview of CSIR-CSIO, express the motivation behind the project, detailed discussion of robots with the objective and software used in this project. An outline and the contributions of the project is presented at the end of the chapter.

1.1 Industry setting

Overview of the organization is given with its past history and its establishments. Also the vision and mission of organization is written and lastly the department in which I have done my internship.

1.1.1 About CSIR

CSIR (Council of scientific and industrial research), India was constituted in 1942 as autonomous body under the provision of the Registration of Societies Act XXI of 1860 [1]. It is among the world's largest publicly funded R&D organization. It has a dynamic network of 38 laboratories, 39 centers, 3 innovation complexes and 5 units [http://www.csir.res.in/about-us/about-csir]. Their activity ranges from aerospace to mining to microelectronics to metallurgy and so on.

1.1.2 CSIR's Vision

"Pursue science which strives for global impact, technology that enables innovation – driven industry and nurture trans-disciplinary leadership thereby catalyzing inclusive economic development for the people of India"[2].

1.1.3 About CSIR-CSIO

Central Scientific Instruments Organization (CSIO), a constituent unit of Council of Scientific & Industrial Research (CSIR), is a premier national laboratory dedicated to research, design and development of scientific and industrial instruments. It is a multi-disciplinary and multi-dimensional apex industrial research & development organization in the country to stimulate growth of Instrument Industry in India covering wide range and applications [3].

CSIO has facilities in the areas of optics and cockpit based instrumentation; biomedical instrumentation; electronics; analytical instrumentation, and mechanical engineering. A large number of instruments have been developed by the CSIO and passed on to the industries for commercial exploitation.

Major R&D areas [4]:

- Strategic and Defense Applications
- Optics & Opto-Electronics
- Computational Instrumentation
- Geo-Scientific Instrumentation
- Medical Instrumentation
- Analytical Instrumentation
- Agri-Electronic Instrumentation
- Energy Management, Condition Monitoring & Quality Control
- Environmental Monitoring Instrumentation
- Micro electro Mechanical Systems (MEMS) and Sensors
- Biomolecular Electronics and Nanotechnology

CSIO has labs available for R&D programmes of the institute. A number of these labs and facilities are used for carrying out research/thesis/project of MTech/PhD level scholars. CSIO has library which has seating capacity of about 40 persons and has around 50,000 books which covers contents of all departments.

1.1.4 Bio-Medical Instrumentation

Bio-Medical Instrumentation is the department under which I have completed my project work. One of the focus areas of research in CSIO is the development of technologies for biomedical

instruments. This department is working towards research, design and development of medical instruments for various purposes like diagnostic, prosthetic, and assistive devices for rehabilitation and orthopedic implants [5].

Various labs of this department are GAIT lab, CARE lab, Metal 3D printing lab and these labs are equipped with technologies like Plastic 3D printing, Force measuring system, Contact angle measurement, Shot-Penning machine and wire cut EDM.

The group has expertise in the following areas:

- Medical Robotics
- Biomechanics
- Machine Vision, Image processing
- Heat Transfer
- Mechanical Design and fabrication, CAD modeling
- Signal processing
- Electronic Design and Control

1.2 History and motivation

The term robot was first introduced into our vocabulary by the Czech playwright Karel Capek in his 1920 play Rossum's Universal Robots, the word robota being the Czech word for work [6]. After that the term has been applied to anything that operates with high degree of autonomy and under computer control.

In the early 1980's, the use of industrial robots has gained popularity. Predictions were that entire factories of the future would be fully automated and will require less number of human workers. And after that production of robots has never stopped and not only in manufacturing industry, robots are now found in many fields, including medical, military and space. When compared to humans, they are more reliable, efficient, and can carry more weight.

With the advancement of technology, manufacturers are now able to reduce cost and increase productivity. For this, there is need to analyze every important aspect which could help in reducing costs and, at same time, will improve efficiency. Manufacturers are looking for the ways to increase the productivity of robots and allowing human operators to focus on other

crucial tasks. Also, there is need to perform different analysis on such robots to help manufacturers minimize production time, travel distance, and/or energy consumed.

1.3 Robots

A robot is an automatically operated mechanism that minimizes human effort and is depicted as very efficient and almost identical to humans except for their lack of emotions. Robots can also be defined as a software controllable mechanical device, having complex mechanical structure and multiple degrees of freedom. We can define robot in many types as they come in different sizes and for different applications. So, as strange as it might seem, there is no standard definition for a robot. However, there are some certain characteristics that a robot should have and will help us to decide whether it is a robot or not or we can say it can help us to decide what features we will need to build a machine that can be called as a robot.

A robot has these essential characteristics:

- **Movement** Based on the application, a robot needs to be able to move around its environment or given workspace. Movement can be in the form of rolling on wheels, walking on legs or propelling by actuators/motors.

- **Energy** For the movement, a robot needs power like solar powered, electrically powered or battery powered. We can choose the way a robot gets its energy only after we know its application.

- **Sensing** For a mechanism to be called as a robot, it should have the ability to sense its surroundings like we humans do i.e. it should be employed with light sensors(eyes), pressure sensors(hands), chemical sensors(nose), sonar sensors(eyes) and taste sensors(tongue).
- **Intelligence** Programming is also very important in the field of robotics to make the robots smart. The programmer will provide the task to the robot and will guide the robot to perform that task effectively and efficiently.

1.4 Robot classification

There are number of configuration of robots but we will discuss some important configuration of robots. Robots can be broadly classified as:

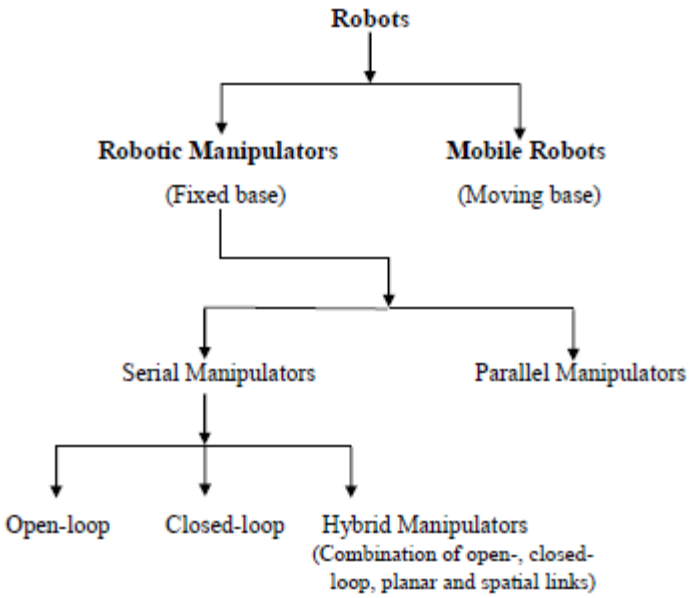

Figure 1.1: Classification of robots

From the above flow chart, robots can be broadly classified as robotic manipulator and mobile robots. The major difference between these two is that in robotic manipulator one of the links, comprising a robotic manipulator, is fixed whereas all the links can move in Cartesian space freely. The link which is fixed is also known as base of robotic manipulator so, if there is a need to change the position of robot in any application than we will use mobile robots. Examples of both are presented in figure 1.2a and 1.2b.

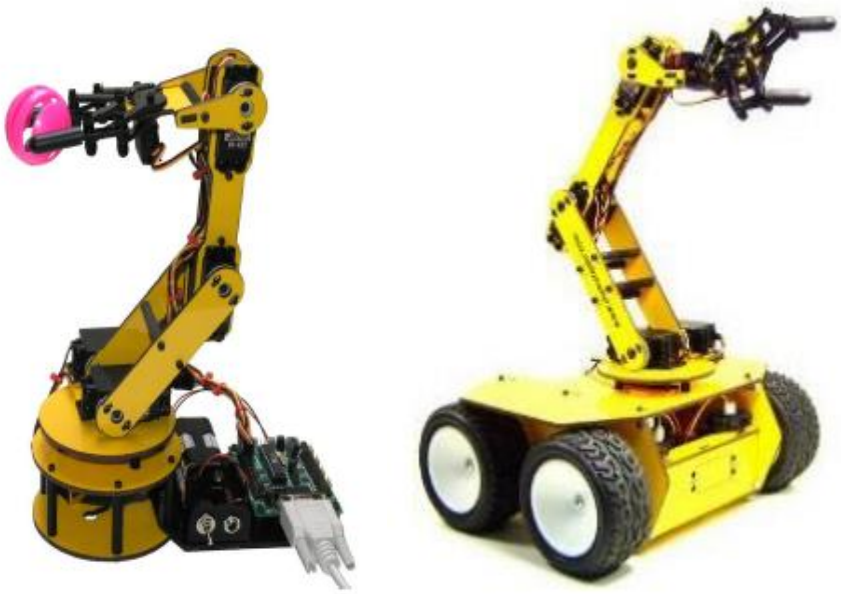

Figure 3.2: Fixed and mobile manipulator [7][8]

1.4.1 Serial Manipulators

Serial manipulators are most commonly used robots in manufacturing industries. They are designed as a series of links i.e. in a progressive sequence, forming an open or closed chain depending upon the type of application. Selecting an open or closed loop chain manipulator is not so difficult, if there is only one required/feasible path to track than open chain manipulator is required for that application, whereas if there are more than one path to reach then it is required to setup closed link manipulator. Open loop manipulators include IRB 140, 6-axis puma 560, 4-axis SCARA robot, Rhino XR-3 etc.

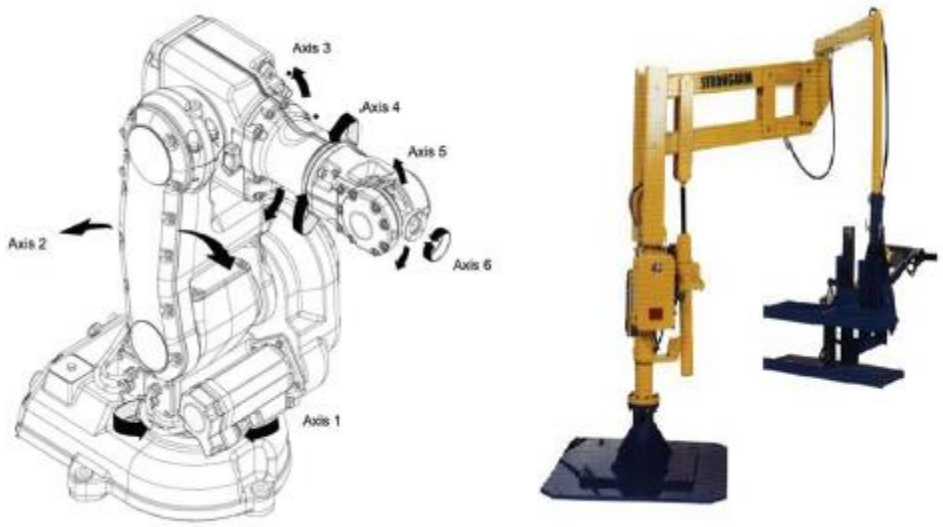

Figure 1.3: Open loop and closed loop manipulator [9][10]

1.4.2 Hybrid manipulators

Hybrid manipulators combine both classes of kinematic chain, namely parallel and serial chain manipulator or open and closed loop chains containing planar and spatial links. These manipulator are modular and can be extended by addition of modules over large distances. Also other advantage is that they offer mechanical advantages where it is possible to locate most of the actuation and transmission systems away from the floating parts of manipulator. But it is difficult to model these manipulators kinematically.

Figure 1.4: A parallel-serial hybrid manipulator [11]

1.5 Objective

The objective of this project is to perform the dynamic analysis of RRR robotic manipulator (include in abbreviations) using ADAMS software and to understand the torque characteristics of the joints for different simulations and selecting the appropriate motors for driving the robotic manipulator in a specified direction. Different approaches are available to simulate the dynamic behavior of robot mechanism but the use of Adams will accurately simulate and diagnose the dynamic performance of the robotic manipulator.

For perfectly diagnose the performance of our model, incorporation of the friction is done by studying the best suited model for our application and also we focused on the theory of Newton-Euler formulation which is a better approach for dynamic modeling of robotic manipulator.

1.6 Software

Following is a short description of the software used for performing the project and why this software is used and the area of utilization.

MSC.ADAMS:

ADAMS [12] stands for Automatic Dynamic Analysis of Mechanical Systems and was originally developed by Mechanical Dynamics Inc.(MDI). MDI was formed by researchers/developers of the original ADAMS code at University of Michigan, Ann Arbor, MI, USA. Later on, it was absorbed into McNeil Schindler Corp (MSC) in 2002.

ADMAS is the most widely used software for the purpose of multi-body dynamics in the world and it has been proved as very essential to Virtual prototype development through reducing product time to market and product development costs.

Base modules are available, inbuilt in the software i.e. Adams/View, Adams/Solver and Adams/Postprocessor and we will be using them for our project.

Chapter 2

Theoretical background

This project will include how a robotic manipulator is interpreted; Fundamental background theory and important notation are explained in this section to facilitate the understanding of the following sections.

Certain concepts/ basics are important to know before modeling and analysis of robotic manipulators. Section (2.1) describes the mathematical modeling of robots i.e. we will be concerned with representing basic geometric and dynamic aspects of robotic manipulation. These ideas will help in developing models of robotic manipulator for any application.

2.1 Symbolic representation of robots

Robot manipulators consist of links connected by revolute or prismatic joints to form a kinematic chain. A revolute joint is like a hinge joint and allows relative rotation between two links i.e. allowing a single degree of freedom while a prismatic joint allows a linear relative motion between two links also allowing a single degree of freedom, thus each joint i can be represented by a single joint variable qi. Figure 2.1 shows a symbolic representation of robot joints in 2D and 3D.

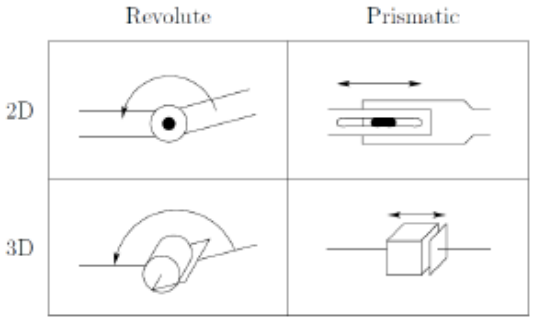

Figure 2.1: Symbolic representation of revolute joints [13].

We will denote revolute joints by R and prismatic joints by P i.e. for example if a robotic manipulator has three revolute joints then it will be called as RRR manipulator.

2.2 Configuration space

For the complete specification of the location of every point of the manipulator i.e. from base of the robot to end effecter, we need a configuration and the set of all configurations is called the configuration space.

Number of DOF determines the dimension of the configuration space and in case of robotic manipulator, number of joints determines the number DOF. A robotic manipulator typically possesses six DOF i.e. three for positioning and three for orientation (e.g., roll, pitch and yaw angles). If a manipulator has less than six DOF then arm cannot reach every point in its environment i.e. it will have limited workspace. Also certain manipulators requires more than six DOF so it will require more than six links and these type of manipulators are called kinematically redundant manipulator.

2.3 The workspace

The workspace of a manipulator is the total volume of space swept out by the end effecter as the manipulator performs all possible tasks. The workspace is limited by the geometry of the manipulator as well as mechanical constraints on the joints. Based on the application of manipulator, workspace can be categorized into reachable and dexterous workspace. The reachable workspace is the entire set of areas reachable by the end effecter of manipulator and the dexterous workspace consists of those points that the manipulator can reach with any arbitrary orientation of the end effecter. For example an articulated manipulator also called a revolute, or RRR manipulator is shown in fig. (2.2)

Figure 4.2: The ABB IRB1400 Robot. Photo courtesy of ABB.

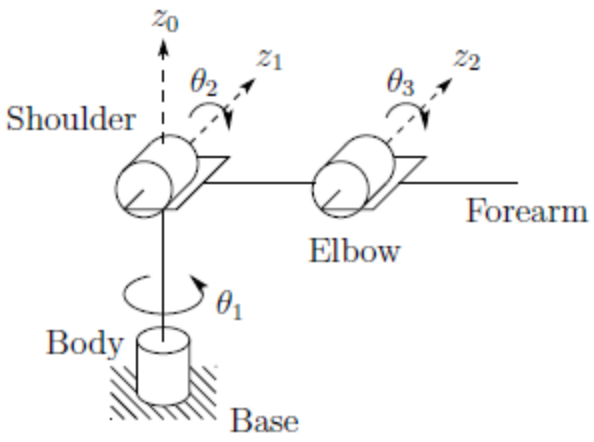

Figure 2.3: Structure of the elbow manipulator.

In these type of arrangement joint axis z2 is parallel to z1 and both z1 and 2 are perpendicular to z0. The structure and terminology liked with this type of manipulator is shown in fig. (2.3) and its workspace is shown in figure (2.4).

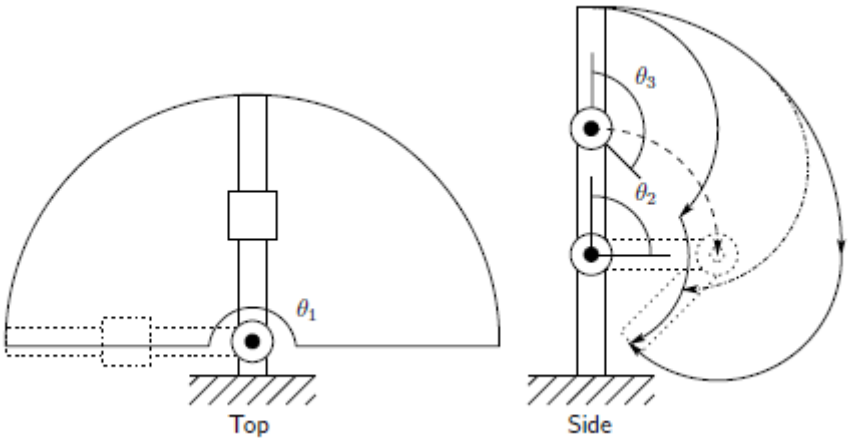

Figure 2.4: Workspace of the elbow manipulator.

Chapter 3

Multi-body modeling of robotic manipulator

3.1 Model design

For understanding the use of MSC ADAMS software for dynamic analysis of multi-body systems we have taken a 3 link robotic manipulator. The model to be built has a base for the support of a pillar from which link 1 is attached with a revolute joint and again link 2 is attached to link 1 using a revolute joint and similarly link 3 is attached with another revolute joint.

3.2 Degree of freedom and joints

Degree of freedom denotes the minimum number of parameters required to completely define the position of entity in space. In 3D space an unconstrained body has six degrees of freedom: three for translations and three for rotations along the three coordinate axes. Constraints reduce the number of degrees of freedom by limiting the bodies' movement. How the mechanism is able to maneuver is directly related to its degree of freedom.
So, our model has 3 D.O.F. as the revolute joints only have one rotational degree of freedom.

3.3 Fix joints

To fix the pillar to the base (ground) we have used the fix joint feature of ADAMS. It locks al the D.O.F. between two bodies. To use a Fix Joint, first two bodies which we want to fix must be selected and also a point where the bodies we want to be locked as shown in figure.

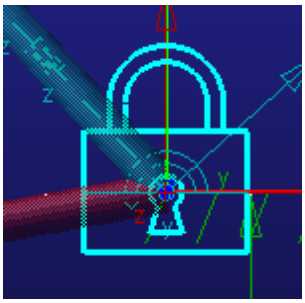

Figure 3.1: Fixed joint

3.4 Markers

Markers in ADAMS are geometrical points with their own local coordinate system. These markers were given a placing relative to each components local coordinate system. The result of this was that they were given a fix placing in the component which then will follow the component in global moving and this was a necessity to get the force actuation to work as desired.

3.5 ADAMS model

After choosing parameters for every part of model we have modeled the 3 link manipulator in MSC ADAMS software as shown in figure 3.2 and for notation, joint connecting the pillar and link1 is joint 1, joint connecting the link1 and link 2 is joint 2 and lastly, the joint connecting the link 2 and end link 3 is joint 3.

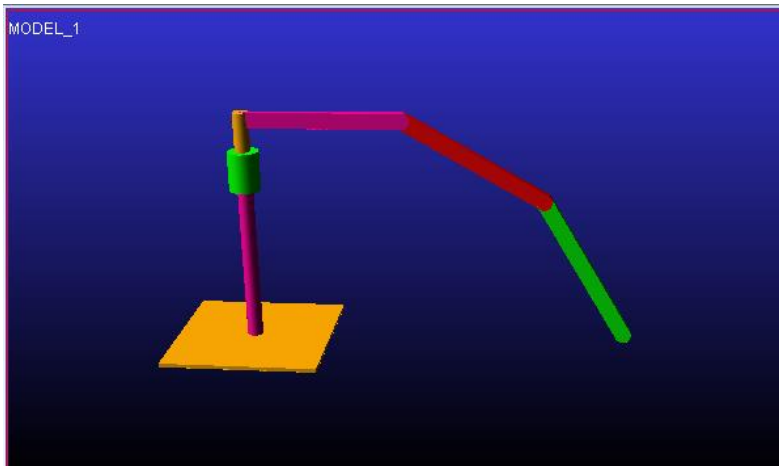

Figure 3.2: Robotic manipulator

The parameters of the 3 link robotic manipulator are shown in the table as follows:

Parts	Dimensions(cm)	Material
Base	20x20x0.5	Steel
Pillar	30x1	Steel
Link1	20x2x1	Steel
Link2	20x2x1	Steel
Link3	20x2x1	Steel

Table 3.1: Parameters of robotic manipulator

Chapter 4

Friction models

Friction is found in every mechanism with moving parts. It is a nonlinear physical phenomenon that is found in almost every system if set in motion, e.g., joints, bearings, transmissions, engines, valves, brakes, and wheels. Friction appears between two surfaces in contact, as well as solids and fluids. If we go in depth then a wide range of physical phenomena causes friction; and it includes elastic and plastic deformations, fluid mechanics and wave phenomena.
Friction should be considered early in the system design by reducing it as much as possible through good hardware design.

4.1 Friction phenomenon

In microscopically point of view, we see the complexities which arries due to friction between two surfaces. Force due to friction is not continuously spread out on the surface, but instead made up by a number of asperities or junctions present on the surface. And as the object will move these contact points will change due to the load, as well as elastic and plastic deformations.

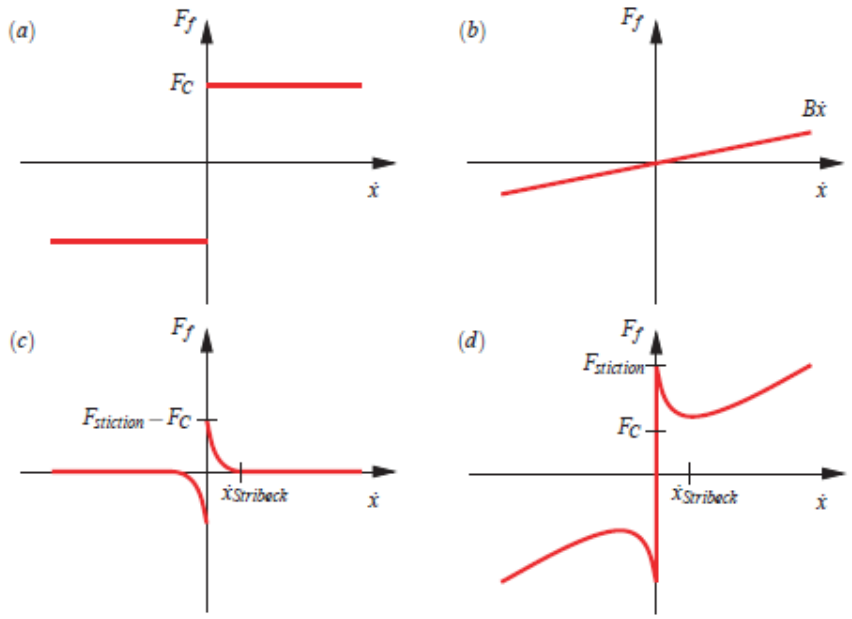

Figure 4.1: Figure illustrating some of the friction contributions and the combined friction.

Coulomb Friction It is a constant friction contribution and thereby not dependent on the velocity as seen in Figure 3.1a.

Viscous friction It is assumed to be almost proportional to the velocity, the viscous friction contribution is expressed as a function of a viscous friction coefficient B multiplied with the velocity as seen in figure 3.1b.

Stribeck friction It is a very important phenomenon and friction phenomenon influencing the operation at low velocities is called the Stribeck effect as shown in figure 3.1c. The Stribeck effect is a friction contribution at low velocities, which is decreasing exponentially from the difference between the stiction (maximum static friction level) and the Coulomb force to zero [14].

Figure 3.1d illustrates the total friction force consisting of the three friction contributions. It is common, in the study of friction, to refer to a curve of the combined friction as a function of velocity by Stribeck friction curve or simply Stribeck curve [14].

4.1.1 Stribeck Friction Regimes

A Stribeck curve illustrates the friction dependence upon velocity. They are often generated by steady state velocity data so behavior of initial friction can be eliminated. The friction seen on the can be divided into four regimes as seen in figure 3.2.

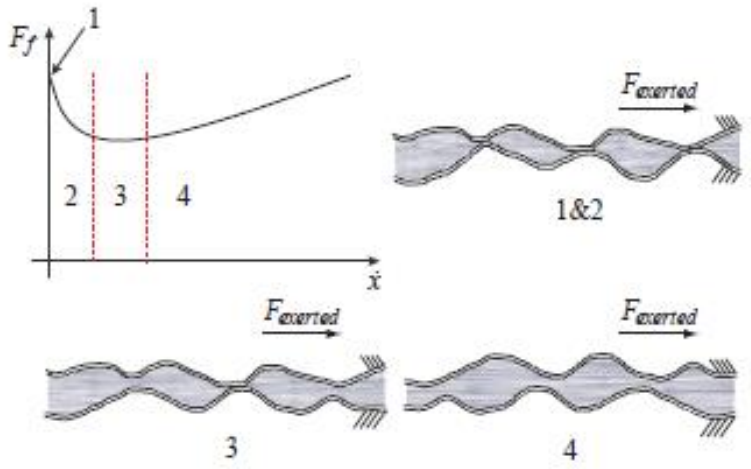

Figure 4.2: Stribeck friction curve divided into four regimes. Modified from [Márton and Lantos, 2006]

The first regime is the stiction, where the surface asperities deform elastically and there is no displacement until the exerted load $F_{exerted}$ reaches the stiction level.

The second regime is the boundary lubrication. Both the stiction and boundary lubrication regimes are solid friction, and the velocity has not yet reached a level where a linear film layer has been developed. The oil is functioning as a lubricant. Boundary lubrication is a process of the shear in the solids, and thus the shear strength normally is greater for solids than fluids the friction is greater than for the third regime, [14].

The third regime is the partial fluid lubrication and in this regime lubrication is forced between the solids by their relatively motion. When the fluid film has grown beyond the height of the aspirates and the load is supported only by the fluid a new regime is entered. This is the full fluid lubrication regime and is the fourth regime where the viscous friction is dominant.
Dynamic viscosity, velocity and contact area determines the friction in the moving object but in the full fluid lubrication regime. This phenomenon is also known as drag force.

4.1.2 Friction Lag

Time lag can be observed in friction when a change in velocity or load force is applied. It can be in milliseconds or in seconds depending on the application. When observing Stribeck curve, a presumption could be made that the friction would be an instantaneously reaction of the velocity. But remember friction always lag velocity [14].

4.1.3 Friction Hysteresis

Friction hysteresis is caused by friction lag and the fact that boundary film layer develops and decreases at different rates depending on the velocity and applied force, amongst other factors. Friction hysteresis is apparent, when the friction force is plotted as a function of the position or velocity of the system, in form of hysteresis loops [15].

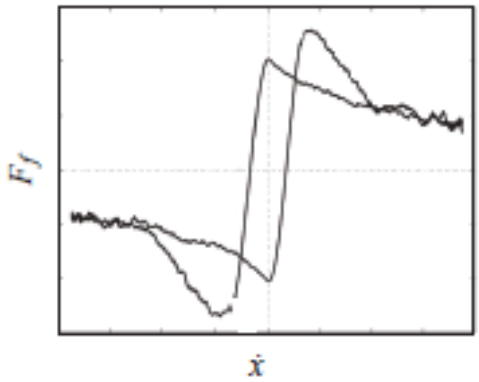

Figure 4.3: A typical rate dependent hysteresis loop. Modified from [Al-Bender, 2005]

4.1.4 Stick Slip motion

Stick-slip motion occurs at close to zero velocity and is apparent in the form of sudden jerking motion. Considering an object at rest on which an external load is applied and increased until the stiction level is reached. As the object starts to move relatively to a surface in contact, the friction transcends from static to dynamic friction level which is, for limited boundary lubrications, a lower value. The external force applied is then decreased until the force is insufficient to sustain the motion and the object is brought to a hold at which point the cycle is repeated. [15].

4.2 Mathematical model of friction

It is very difficult to formulate a complete mathematical model that captures all the friction phenomena seen in the previous section as it involves theory from so many different areas. The choice of friction model is dependent on the purpose of the friction model and how it will be used. The friction models which we have chosen includes dynamics in order to accurately describe the friction phenomena as the static models have proven to be insufficient.

4.2.1 LuGre model

This friction model offers a good compromise between complexity and accuracy. It covers the main phenomena of friction, i.e., Coulomb friction, viscous friction, static friction, Stribeck effect, as well as the dynamic properties, such as hysteresis, pre-sliding displacement, and varying break-away force.

The asperity junctions are in the LuGre model considered as bristles which is illustrated in figure 3.14. For simplicity, the bristles in one of the two, relative to each other, moving surfaces are modeled as rigid and the bristles on other surface are modeled as elastic.

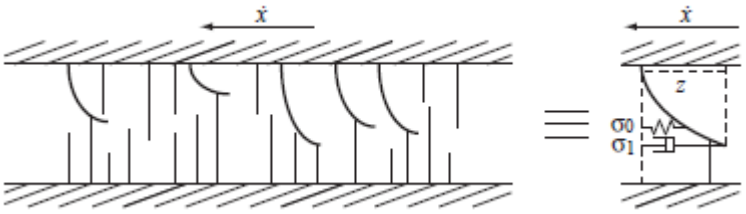

Figure 4.4: Bristle modeling.

The parameter σ1 is the micro-viscous coefficient which is equivalent to a damping coefficient. The parameter σ0 is the average stiffness of the bristles.

The average deflection of the deformable elastic bristles is denoted by z and the rate of deflection z is modeled by equation

$$\dot{z} = \dot{x} - \frac{\dot{x}}{g(\dot{x})} z$$

Where,

$$g(\dot{x}) = \frac{1}{\sigma 0} (Fc + (F_{stiction} - Fc) e^{-\left(\frac{\dot{x}}{\dot{x}_{stribeck}}\right)})$$

Where δ is an arbitrary constant which is geometry dependent and often set to unity. The steady state deflection z.ss is described by equation

$$z_{ss} = sign(\dot{x}) g(\dot{x})$$

The friction force generated when bending the bristles is described by equation

$$F_{f,bristles} = \sigma_0 z + \sigma_1 \dot{z}$$

The final LuGre model emerges when adding the viscous friction term B x to equation shown above is presented in equation

$$F_f = \sigma_0 z + \sigma_1 \dot{z} + B\dot{x}$$

Note the steady state friction force $F_{f,ss}$ arises when the velocity $\dot{x}$ is held constant and can be expressed by equation

$$F_{f,ss} = sign(\dot{x})[F_c + (F_{stiction} - F_c) e^{-\left(\frac{\dot{x}}{\dot{x}_{stribeck}}\right)}] + B\dot{x}$$

And, values of friction parameters were taken from literature as given below: [16]

Friction parameters	v>0	V<0	Nominal values
α_0	0.28	0.29	0.285
α_1	0.06	0.04	0.05
α_2	0.0176	0.0189	0.018
v_0	0.01	0.01	0.01
σ_0	-	-	260.0
σ_1	-	-	0.6

So, by putting these values and value of angular velocity of any joint, in above equation we can get an estimate value of the friction torque value.

Chapter 5

Adding motion to robotic manipulator

5.1 Applying ADAMS electric motor at joints

In order to move the robotic arm we need to apply torque at the joints; for this we have used ADAMS/machinery electric motor module which is fully incorporated inside the ADAMS/ view environment.

In this module we can choose different modeling method for different applications. So, we have used analytical method and in this we have DDC (shunt or series), DC brushes, and stepper and AC synchronous motors and for our application we have used stepper motor.

Stepper motor is a brushless, synchronous electric motor that converts digital pulses into mechanical shaft rotation. Stepper motor is used whenever we want controlled rotation or precise angular rotation without the use of feedback sensors. [17]

We have modeled the motor by specifying motor geometry i.e. dimensions of rotor and stator and input parameters like holding torque, step angle, friction torque, damping coefficient.

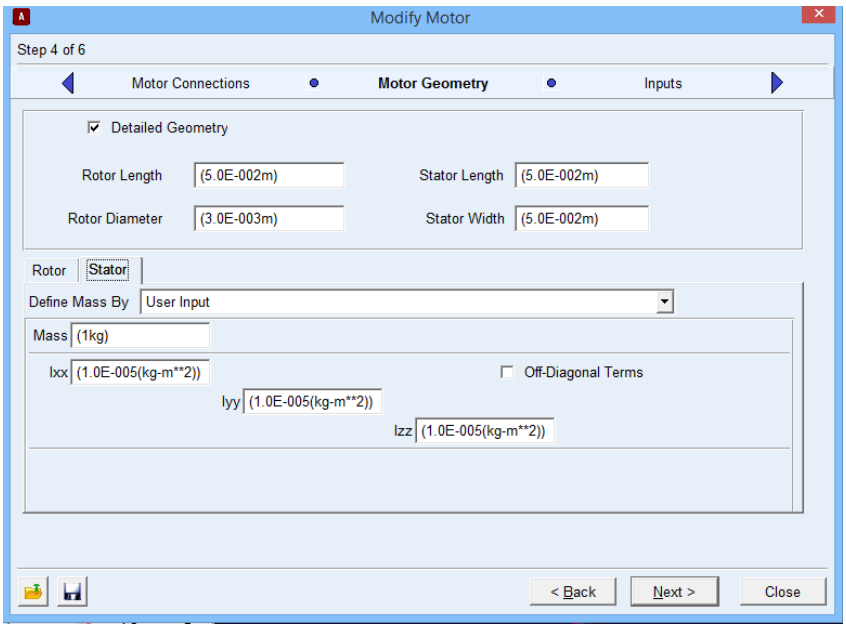

(a): Motor geometry

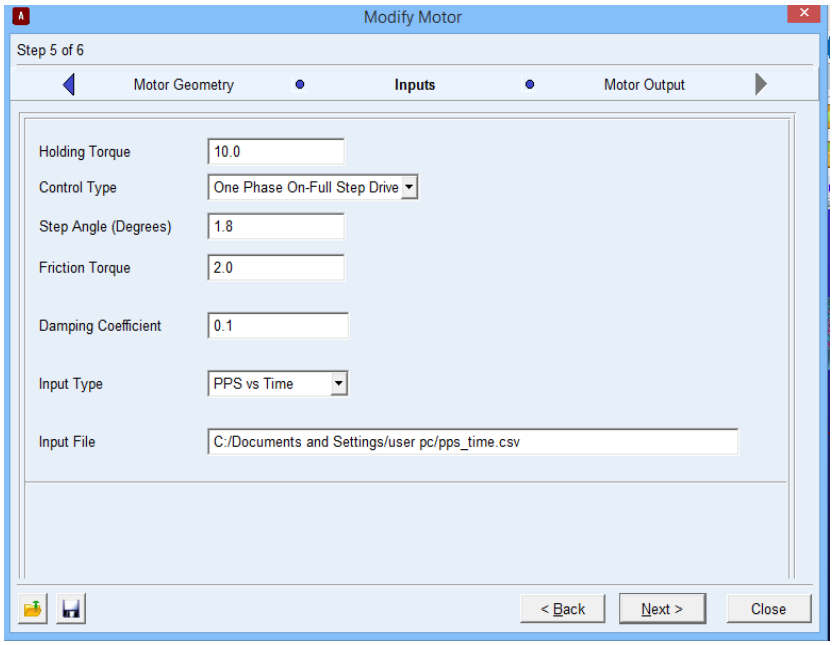

(b): Specifying input parameter

Figure5.1: Modeling of electric motor in ADAMS platform

5.2 Applying joint motion

There is also another way of moving robotic arm i.e. by using ADAMS motion feature.

In this we specify the two bodies on which we want to impose motion and a point where we want torque to act.

We will be considering two cases first will apply joint motion with no weight attached at joints and other case would be a weight attached at joints so that we can get result close to real case scenario. For our simplicity we have used cylindrical part at joints with cross-section (5x1) cm and with material as Steel.

The links were rotated by applying joint motion given under motion tab and motion is determined with STEP function. The STEP-function is given an initial condition, an end condition, and the timeframe during which the force is varied, as seen in Figure 6.2. The function then returns a value which is calculated with one of the function pieces, in this case the variation of the force is calculated with a cubic polynomial.

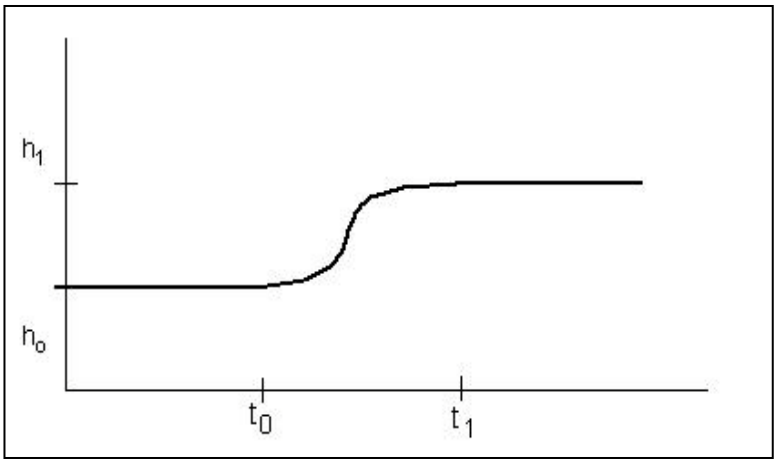

Figure 5.2: Illustration of the STEP function

Mathematically, the STEP-function operates according to [16]

$$a = h_0 - h_1$$

$$\Delta = \frac{(t - t_0)}{(t_1 - t_0)}$$

$$\text{STEP} = f(t) = \begin{cases} h_0, t \le t_0 \\ h_0 - a \cdot \Delta^2(3 - 2\Delta), t_0 < t < t_1 \\ h_1, t \ge t_1 \end{cases}$$

Where t is time, h_0 is the initial condition, and h_1 is the end condition. This function can then be changed between each simulation to create a certain combination of movements of joints.
In our project, we want to analyze the torque at each joint when it rotates clockwise and anti-clockwise for let say n degree angle rotation so for this we have used step function as;

- For clockwise- Displacement = STEP (time, t_0, h_0, t_1, nd)
- For anti-clockwise- Displacement = STEP (time, t_0, h_0, t_1,-nd)

5.3 Adding general motion

For movement of end effecter i.e. end point of link 3 of robotic manipulator, general motions feature is given in ADAMS/View.

There are two tabs given under this feature which are:

- Single point motion
- General point motion

Single point motion includes adding motion to two parts along or around one axis and general point motion includes adding motion to two parts along or around the three axes.
So, to apply this feature, we have to specify parts to which the motion is to be applied and the location and orientation of the motion. As shown in figure 6.3, we have applied single point motion to the end effecter i.e. end point of link 3 and in the upward direction i.e. along z axis. Now, Adams will attach markers on each part at the location of the motion but in our case we have selected only one point for motion, so, Adams will automatically attach other marker at ground and this will act as a reference point while other point where first marker is created is called moving point.

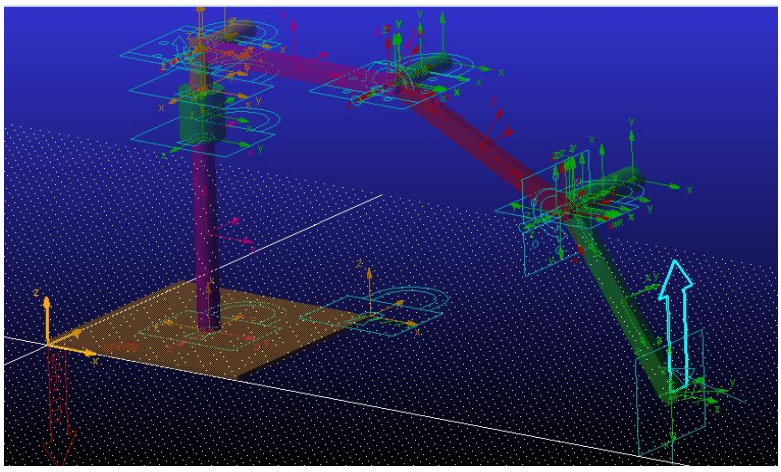

Figure 5.3: Adding general motion to end effecter

Also, before adding motion to the end effecter we need to constrain our end effecter otherwise it will show error and we will not be getting trajectory according to input equation. So, we have to add In-plane primitive joint, this feature will constrain the selected joint in one plane but in our case its point so Adams will take this point and constrain this point in a plane with ground.

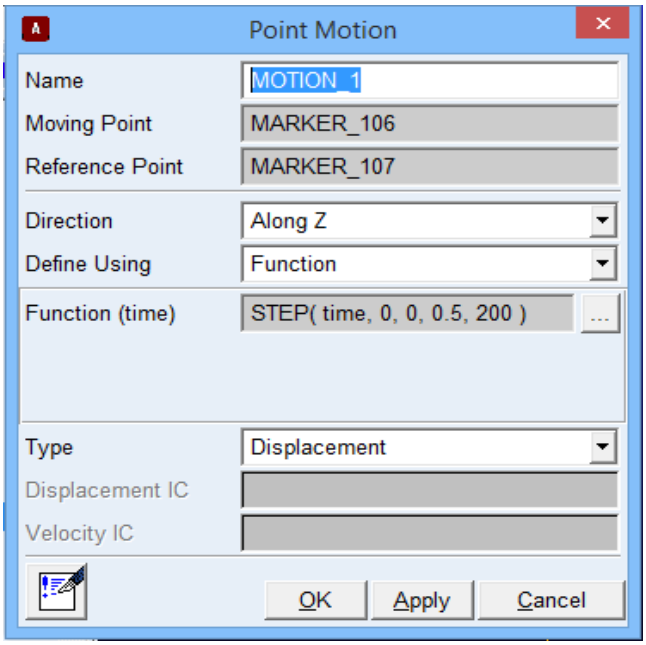

Figure 5.4: Adding point motion palette

Now, after adding constraint and specifying direction of motion to end effecter, we need to input function which will define the movement of end effecter in time and here also we are using STEP function because it can give smooth movement to end effecter in given time period (Refer to section 4.2 for theory of this function) .

Chapter 6

Drive System design

Drive system design is a crucial component in designing of robotic manipulator and it consists of several parameters which are needed to be determined:

- Motor allocations,
- Motor choice and sizing,
- Gearbox choice and sizing.

In the first stage of drive system design, motor allocation is performed and after that motor and gearbox sizing is done based on torque requirements, and are chosen from Maxon Motor catalog.

6.1 Motor allocations and Transmission Systems

Actuators of RRR manipulators with open-chain configuration are generally located contiguous to the joints i.e. direct drive is implemented on every joint. But we can allocate motor to other position also and for deciding the position of allocation of motors we need to look into different transmission systems which are used to drive links.

There are mainly three different articulated manipulators in terms of transmission systems as shown in figure 6.1

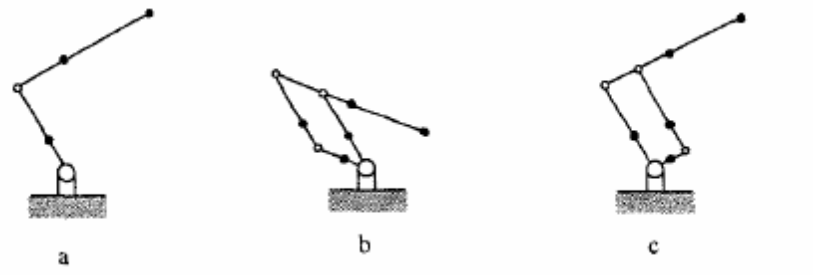

Figure 6.1: Different configuration of articulated manipulator

Figure 6.1a shows the joint manipulator which is an open-linkage arm, figure 6.1b, 6.1c shows parallelogram and Gopalswamy's manipulator respectively and they are closed-linkage arms.
Choice of transmission system depends on the power requirements, desired motion, and speed. In our case we want low speed of end effecter and less complexity on joints as after choosing closed-linkage arms we will add more complexity so direct drive is suitable for our case and there are other benefits of choosing direct drive which are:

- It eliminates backlash and mechanical deficiencies like friction and compliance.
- Its eliminates the need of a power transmission thus making the manipulator more efficient
- Joint back drivable i.e. allowing for joint space force sensing.

6.2 Motor selection

In this section we will discuss the motor selection. First the requirements will be discussed and available motors will be explained. Then we will choose the motor based on our requirements.

6.2.1 Requirements

There are several requirements for the motor to be selected. Majorly we will look for the torque requirements of the robotic arm before sizing the motor and these requirements are:

- For every joint, one motor will be used and in our case we will select three motors as we have three revolute joints.
- A motor needs to deliver the specified amount of torque to the joint in motion and it should work under operating range.
- The power consumption should be kept as low as possible.
- Only one type of motor should be selected for every joint in a robotic manipulator, to keep the system modular.

The motor will move every single joint to make the robot end effecter move in a specified direction. This means that every motor has to deliver a torque great enough to lift the part of the arm after the joint. So, if a lightweight motor is chosen, this will reduce the torque needed by every single joint because if the motor will be light then less weight will be there at every joint.

Also it is important to keep the power consumption low. Since the joints have to be kept modular and simple, we will select only one type of motor.

6.2.2 Types of motor

There are number of electric motors are available in the market, but the brushed DC motor, brushless DC motor and stepper motor are used most commonly in robotic design [19] Some other types of motor are available in market like induction motor (asynchronous AC motor) [20] The motor that will be discussed are given below:

- Brushed DC motors
- Brushless DC motors
- Stepper motors
- Induction motors

Brushed DC motors The brushed dc motors are powered by direct current power source and are internally commutated. They consists of stator and rotor in which stator contains fixed electromagnet or any permanent magnet and other rotor contains an armature with a set of windings. Brushes in this type of motor make mechanical contacts with electrical contacts on the rotor.

Brushless DC motors With this type of DC motor, a type of synchronous motor, brushes are removed by an external controller element. This means that, coils can now be placed inside the stator around the rotor. The advantage is that it improves the heat transport to the outside of the motor.

Stepper motor The stepper motor is also a type of synchronous motor, which only takes discrete steps. This means that the rotation is divided into large number of small even steps. The steps taken by stepper motor are smaller than steps taken by brushless motor and hence give precise control.

Induction motor Induction motor operates on an AC current and it is also called asynchronous motor or AC motor. The working of this motor is that it rotates due to the slip generated by the

difference in phase of the rotor and the phase of the stator field. However the starting torque is low as a result of a non-linearity between the torque and speed. When the motor starts, it draws a large current which results in a voltage drop on the supply line. When light loads are applied to the joint, the power factor decreases significantly, this reduces the efficiency of the motor [21].

So, after taking everything into account we agreed to take brushed DC motor because we don't need any electronics to run the motor and also offering a unique plug-and-play option to the designer. The brushed motor will save the overall cost of the system and as the development costs increase and quantities tend to decrease, it is important to select brushed DC motor.

6.2.3 Motor selection criteria

For selecting the right motor we will use the online Maxon Motor catalog and the following constraints must not be violated

Nominal torque limit The maximum continues torque is called nominal torque. For this condition, the root mean square (RMS) value τ_{rms} of the required motor torque τ_m has to be smaller than or equal to the nominal torque of motor i.e. T_m

$$\tau_{rms} \leq T_m$$

where $\tau_{rms} = \sqrt{\frac{1}{\Delta t}\int_0^{\Delta t} {\tau_m}^2 dt}$, with Δt being the duration of a working cycle of the motor.

Stall torque limit The peak torque of motor is called stall torque of the motor. The required peak torque τ_p has to be smaller than or equal to the stall torque T_m^{max} of the motor

$$\tau_p \leq T_m^{max}$$

where $\tau_p = \max\{|\tau_m|\}$.

Maximum permissible speed limit The commutation system generally limits the maximum permissible speed limit for DC motors. The required peak speed n_p corresponding to the motor has to be smaller than or equal to the maximum permissible speed N_m^{max} of the motor

$$n_p \leq N_m^{max}$$

where$n_p = \max\{|2\pi\dot{\theta}(t) \cdot \rho|\}$.

The given equations represents the constraints that must not be violated by any motor chosen for operation in any application.

6.3 Gearhead selection

In this section we will discuss the gearhead selection. First the available gearhead will be explained. Then we will choose the gearhead based on our requirements.

6.3.1 Types of Gearhead

If mechanical power is required at a high torque and correspondingly reduced speed, a precision gear is recommended [22]. Motors with built-in gearhead can provide a more cost-effective solution as assembling separate components will require more money. The gear head that will be discussed are given below:

- Spur gearhead
- Planetary gearhead

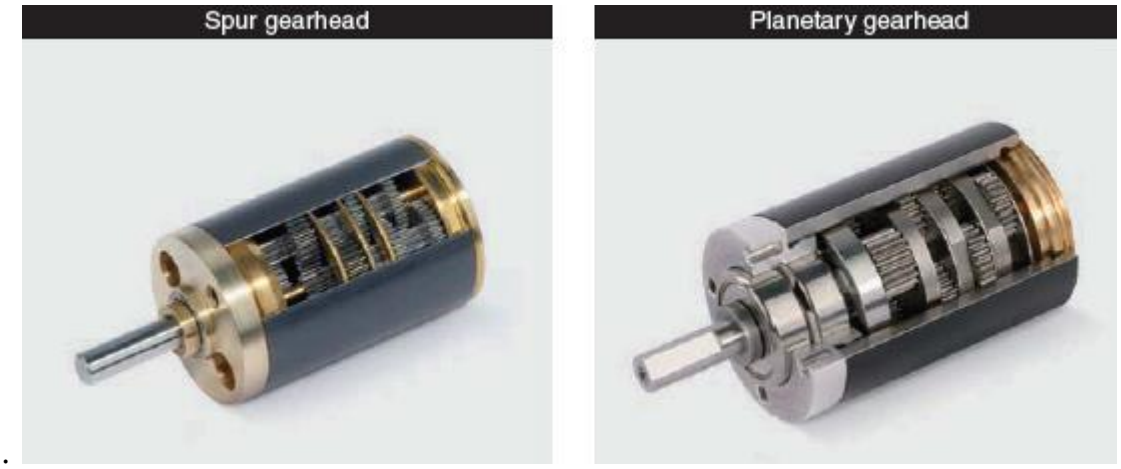

Figure 6.2: Spur and planter gearhead

Determining the type gear head to be used depends upon the number of factors such as backlash, efficiency, speed, reduction ratio and cost. Spur gearhead are simple and less expensive but they work for only low-torque applications and planetary gearhead work for wide range of torque.
Torque capacities of spur gearhead are limited because each gear bears entire load. In planetary gears, load is distributed over multiple gears i.e. central sun gear is driven by input shaft and it

drives the other planet gears. So, by keeping all these things in mind we selected planetary gear head for our application for each and every joint to be driven.

6.3.2 Gearhead selection criteria

Same as the motor selection criteria, in the selection of the gearhead, the following constraints are considered that must not be violated:

Maximum output torque limit The required peak torque τ_g with respect to the output side has to be smaller than or equal to the allowable peak torque T_g^{max} of the gear drive

$$\tau_g \leq T_g^{max}$$

where $\tau_g = \max\{|\tau_g|\}$.

Maximum permissible input speed limit The required maximum input peak speed n_{in} has to be smaller than or equal to the maximum permissible input speed N_g^{max} of a gearbox

$$n_{in} \leq N_g^{max}$$

$n_{in} = \max\{|\dot{\theta}(t) \cdot \rho|\}$.

The given equations ( ) to ( ) represents the constraints that must not be violated by any gear head chosen for operation in any application.

Also, after choosing the gear head we need to convert the speed and torque of the gear output to the motor shaft

$$n_m = i \cdot n_g$$

$$T_m = \frac{T_g}{i \cdot \eta_G}$$

Where:

i: reduction

η_G: Gearhead efficiency

Chapter 7

Dynamic modeling of robotic manipulator in general

Serial manipulators can be described mathematically in different ways. Robot kinematics deals with the motion of the manipulator without considering forces and torques causing the motion. The focus of kinematic analysis is in two areas i.e. forward and inverse kinematics. Forward kinematics deals with computing the position and orientation of end effecter relative to the base when joint angles of the manipulator are given and inverse kinematics being the more difficult converse problem, deals with computing the set of joint angles which will achieve the given desired position and orientation of the end effecter or tool relative to user's workstation or base of a manipulator. But in this area, forces are not considered that causes motion and that's why we have to look at more advance area i.e. robot dynamics and in this section, we will be discussing this area in depth.

Dynamic modeling means deriving equations that formulate the relationship between forces and motion. These equations are necessary to consider for simulations and control algorithm design.

Our study of robotic manipulator so far has focused on analysis of robotic manipulator using ADAMS software. We have studied variation of joint torque with different conditions imposed on manipulator; but we have never thought of the governing equations of motion of manipulator. So, now we will deduce the equations of motion of manipulator in general- the way in which motion of any serial manipulator arises from torques applied by the actuators or from external forces.

7.1 Different approaches

Computing the dynamic equations of manipulator can be quite challenging. Researchers have discovered two basic approaches, namely Newton-Euler formulation and Euler-Lagrange formulation where former is based on "force balance" approach to dynamics and later is an "Energy-based" approach to dynamics. In the Euler-Lagrange formulation the manipulator is treated as a whole, and the system is analyzed based on its kinetic and potential energy. The

Newton-Euler formulation is quite different because each link of the manipulator is isolated first and then dynamic equations are written for every link isolated. But the resultant dynamic model is the same for both methods and can be written in matrix form as

$$M(\theta)\ddot{\theta} + V\left(\theta, \dot{\theta}\right) + G(\theta) = \tau$$

Where

θ = joint variables vector

u = Resultant torque vector

M = inertia matrix

V = centrifugal and Coriolis terms

G = gravity vector

7.2 Background theory and notation

This section will give the background theory of the derivation of the Newton-Euler formulation and it will be important to understand before going towards the derivation.

7.2.1 The Rotation Matrix

In order to perform the algebraic manipulations with different frames, we need to express them in same coordinate frame. Here comes the role of rotation matrix which can be written as

$$R_1^0 = [x_1^0 \quad y_1^0 \quad z_1^0]$$

Where the columns are the coordinates of the vector $\mathrm{x}_1, \mathrm{y}_1$ and z_1 expressed in frame 0.

Now, vectors are denoted with a superscript to show the frame in which they are expressed. Now, if we want the relationship between the same vectors in different reference frame, it will be shown as

$$\mathrm{v}^0 = \mathrm{R}_0^1 \mathrm{v}^1$$

$$\mathrm{v}^1 = \mathrm{R}_2^1 \mathrm{v}^2$$

$$\mathrm{v}^0 = \mathrm{R}_0^2 \mathrm{v}^2$$

which gives

$$\mathrm{R}_2^0 = \mathrm{R}_1^0 \mathrm{R}_2^1$$

7.3 Newton-Euler formulation

In this section, we will derive equations of the Newton-Euler formulation which can be applied to any number of links attached to a serial manipulator.
The following derivation of the Newton-Euler formulation is entirely based on the derivation presented in [23].

7.3.1 The General Case

Three important laws form the basis of the Newton-Euler formulation:

- Newton's third law states that for every action there is an equal and opposite reaction. Thus, if link 1 applies a force f and torque τ to link 2, and then link 2 applies force and torque of same magnitude but in opposite direction.
- The rate of change of the linear momentum equals the total force applied to the link.
- The rate of change of the angular momentum equals the total torque applied to the link.

Applying the second law to the linear motion of a link gives the relationship

$$\frac{d(mv_c)}{dt} = f$$

where m is the mass of the link, v_c is the velocity of the center of mass with respect to an inertial frame, and f is the sum of forces acting at C.O.M. of the link.

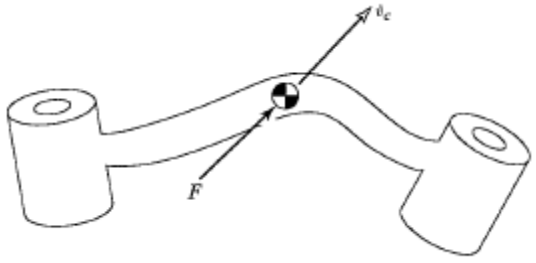

Figure 7.1: Force acting the COM of the link

Above equation can be simplified to

$$f = m * \dot{v}_c$$

where $\dot{v}_c$ is the acceleration of the center of mass.

The third law gives the relationship

$$\frac{d(I_0\omega_0)}{dt} = \tau_0$$

where $I_0$is the moment of inertia of the link, ω_0 is the angular velocity of the link, and τ_0 is the sum of torques applied on the link. All three variables are expressed in an inertial frame whose origin is at the center of mass. Now, as the link is the link is rotating and we know that I_0 is not a constant function of time, so we can transform it to instantaneous function inertia tensor which will be valid for frame attached to the link instead of an inertial frame i.e.

$$I = R^{-1}I_0R$$

which gives

$$I_0 = RIR^T$$

where R is the rotation matrix that transforms coordinates from the frame attached to the link to the inertial frame. Above equation together with

$$\omega_0 = R\omega, \qquad \tau_0 = R\tau$$

yields,

$$\frac{d(I_0\omega_0)}{dt} = \frac{d(RIR^TR\omega)}{dt}$$
$$= \frac{d(RI\omega)}{dt}$$
$$= \dot{R}I\omega + RI\dot{\omega}$$

and the equation for the rate of change of the angular momentum with respect to the link attached frame is

$$\tau = R^T\tau_0$$
$$= R^T(RI\omega + \dot{RI\omega})$$
$$= R^T\dot{R}I\omega + I\dot{\omega}$$

The final torque expression becomes

$$\tau = R^T \dot{R} I\omega + I\dot{\omega}$$
$$= R^T S(\omega_0) R I\omega + I\dot{\omega}$$
$$= S(R^T \omega_0) I\omega + I\dot{\omega}$$
$$= S(\omega) I\omega + I\dot{\omega}$$
$$= \omega \times (I\omega) + I\dot{\omega}$$

So, force and torque balance equations are

$$f = m * a$$
$$\tau = \omega \times (I\omega) + I\dot{\omega}$$

7.3.2 Equation of n-link Manipulator

Now, derivation of the Newton-Euler formulation requires a set procedure to be followed which includes

- Considering every link as isolated and writing dynamic equation for every isolated link.
- Do outward iterations to compute velocities and accelerations.
- Then, inward iterations to calculate forces and torques.

Now, we will consider the problem of computing the joint torques of n-link manipulator that correspond to a given trajectory and this will help us to get better understanding of torque characteristics of each joint after performing simulations.

In order to compute the inertial forces acting on the link, it is necessary to calculate the linear and rotational velocities and accelerations of each link. To begin with, several vectors need to be introduced and we will always use link frame {0} as our reference frame and all vectors are expressed in frame {i}.

v_i^i= Linear velocity of origin of link frame {i} with respect to frame {i}

ω_i^i= Angular velocity of link frame {i} with respect to frame {i}

v_{i+1}^i= Linear velocity of origin of link frame {i+1} with respect to frame {i}

ω_{i+1}^{i}= Angular velocity of link frame {i+1} with respect to frame {i}

P_{i+1}^{i}= Position vector that locates the origin of link i+1 with respect to link i.

R_{i+1}^{i}= Transformation of coordinates of link frame {i+1} with respect to link frame {i}.

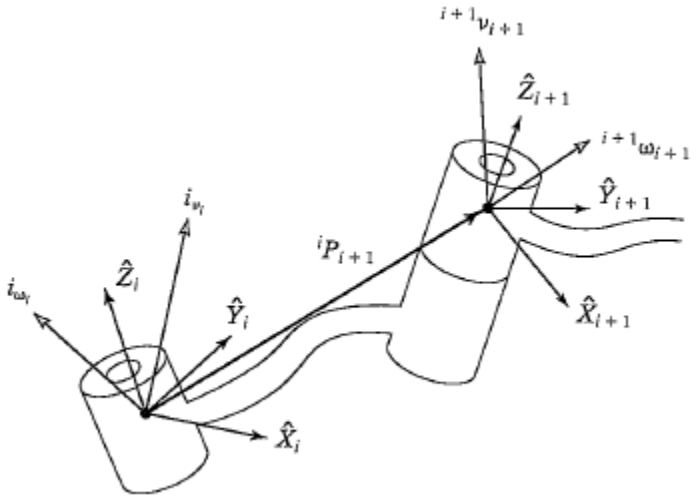

Figure 7.2: Various Vectors acting at the link

Figure 8.2 shows the link i and i+1, along with the linear and angular velocity vectors defined in their link frames.

Now, we will compute the angular velocity of link i+1 and rotational velocities can be added when both ω vectors are written with respect to the same frame. Therefore, angular velocity of link i+1 is equal to the angular velocity of link i plus a new component due to rotation of joint i+1. This can be written in terms of frame {i} as

$$\omega_{i+1}^{i} = \omega_{i}^{i} + R_{i+1}^{i}\dot{\theta}_{\iota+1}\dot{\hat{Z}}_{\iota+1}^{\iota+1}$$

Also,

$$\dot{\theta}_{i+1}\hat{Z}_{i+1}^{i+1} = i+1\begin{bmatrix}0\\0\\\dot{\theta}_{i+1}\end{bmatrix}$$

So, for representing angular velocity of link i+1 with respect to frame {i+1} we have to multiply R_{i}^{i+1} to equation(),

$$\omega_{i+1}^{i+1} = R_{i}^{i+1}\omega_{i}^{i} + \dot{\theta}_{\iota+1}\dot{\hat{Z}}_{\iota+1}^{\iota+1}$$

Similarly, to compute linear velocity of the origin of frame {i+1} we have to add linear velocity of origin of frame {i} linear velocity due to rotation of link i i.e.,

$$v_{i+1}^{i} = v_{i}^{i} + \omega_{i}^{i} \times P_{i+1}^{i}$$

Again, multiplying both sides by R_i^{i+1}, we get

$$v_{i+1}^{i+1} = R_{i}^{i+1}(v_{i}^{i} + \omega_{i}^{i} \times P_{i+1}^{i})$$

Now, in order to compute the angular acceleration we will be using equation( ) to transform angular acceleration from one link to another:

$$\dot{\omega}_{i+1}^{i+1} R_{i}^{i+1} \dot{\omega}_{i}^{i} R_{i}^{i+1} \omega_{i}^{i} \dot{\theta_{\iota+1}} \hat{Z}_{i+1}^{i+1} \ddot{\theta_{\iota+1}} \hat{Z}_{i+1}^{i+1}$$

From above equation, we obtain the equation for transforming linear acceleration from one link to next:

$$\dot{v}_{i+1}^{i+1} = R_{i}^{i+1}[\omega_{i}^{i} \times P_{i+1}^{i} + \omega_{i}^{i} \times (\omega_{i}^{i} \times P_{i+1}^{i}) + \dot{v}_{i}^{i}]$$

Same equation, can be used to compute linear acceleration of the centre of mass of each link:

$$\dot{v}_{C_i}^{i} = \dot{\omega}_{i}^{i} \times P_{C_i}^{i} + \omega_{i}^{i} \times (\omega_{i}^{i} + P_{C_i}^{i}) + \dot{v}_{i}^{i}]$$

Now, we have computed everything required to calculate inertial forces and torque acting at the centre of mass of the link. Thus we have

$$F_i = m\dot{v}_{C_i}$$
$$N_i = I^{C_i}\dot{\omega}_{\iota} + \dot{\omega_{\iota}} \times I^{C_\iota}\omega_{\iota}$$

Where $\{C_i\}$ has its origin at the centre of mass of the link and has the same orientation as the link frame, {i}.

To find the joint torques that will result in these net forces and torques, we have to write force-balance and moment- balance equation based on a free- body diagram of a link. From figure( ), we can see that each link exerts a force and torque on its neighboring link and also experiences an inertial force and torque i.e.

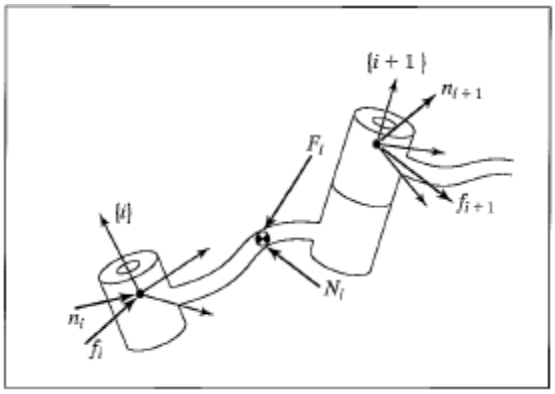

Figure 7.3: Torque and force acting at the COM

$$F_i^i = f_i^i - R_{i+1}^i f_{i+1}^{i+1}$$

$$N_i^i = n_i^i - n_{i+1}^i + \left(-P_{C_i}^i\right) \times f_i^i - (P_{i+1}^i - P_{C_i}^i) \times f_{i+1}^i$$

or,

$$N_i^i = n_i^i - R_{i+1}^i n_{i+1}^{i+1} - \left(P_{C_i}^i\right) \times F_i^i - P_{i+1}^i \times R_{i+1}^i f_{i+1}^{i+1}$$

where,

f_i= force exerted on link i by ink i-1,

n_i= torque exerted on link i by ink i-1.

Finally, we can rearrange equation as,

$$f_i^i = F_i^i + R_{i+1}^i f_{i+1}^{i+1}$$

$$n_i^i = N_i^i + R_{i+1}^i n_{i+1}^{i+1} + \left(P_{C_i}^i\right) \times F_i^i + P_{i+1}^i \times R_{i+1}^i f_{i+1}^{i+1}$$

Required joint torque is the $\hat{Z}$ component of the torque applied by one link on its neighbor:

$$\tau_i = n_i^{i^T} \hat{Z}_i^i$$

Chapter 8

Results and Discussion

This chapter deals with simulations of the robotic manipulator with different constraints set to the joints, links and to the end effecter and plotting the required results and lastly the discussion of every result generated. Note that the goal is to prove the validity of the model by doing simulations and to build the realistic model by adding motor and friction to the joints.
Simulation types are discussed in section 9.1 where we will point out the importance of dynamic simulation. ADAMS measure function is discussed in section 9.2 as this function will be used throughout in generating plots.

8.1 Simulation Types

Adams lets you build and test virtual prototypes, realistically simulating on your computer, both visually and mathematically, the full motion behavior of your complex mechanical system design and it offers multiple types of simulations, and many tools to help build models as accurately as possible.
The kinematic mode is applicable when there are zero degrees of freedom. Any movement in the system is done by forced motions at joints and there are no freely moving parts. In this mode, ADAMS uncouples the motion and force equations and first solves positions, then velocities, accelerations and forces algebraically [24][25].
In static mode, whole system should be in equilibrium at independent time steps and reaction forces are determined so that they balance out the external forces. Equilibrium means that all external velocities and accelerations are zero and no movement is experienced by that system. This mode is useful only if inertial effects are not taken into account. Before going for a dynamic simulation, static needs to be determined. For example, in vehicle simulation it is important to place the vehicle on the ground before attempting a dynamic simulation [24].
When the system has more than one degree of freedom, a dynamic analysis is required. In dynamic simulation, the differential equations are automatically formulated and numerically

solved to determine the system's components' positions, velocities, accelerations and forces.[24] The simulations are all done at predetermined time steps, known as integration time steps. The step size is free for user to select though the program may compute additional time points between the steps. The user also sets a simulation stop time, that is, the time limit how long the simulation is run [24].

8.2 Measures

ADAMS has an inbuilt feature to continuously measure the angles of the joints that are changing during simulation. These functions are measuring the angle between exactly three points and the values of these Measures that can be generated by exporting plots in excel, can be used continuously to control the magnitude of the forces. They are applied by selecting three points, where the second point will become the placement of the angle measure. Measures have the ability to plot the position of an object, the magnitude of any force, or a user defined function generated in ADAMS platform.

8.3 Rotation of joint 2:

Firstly, joint 2 is rotated clockwise and anti- clockwise while other joints are kept fixed by changing their feature from revolute joint to fixed joint as shown in fig.

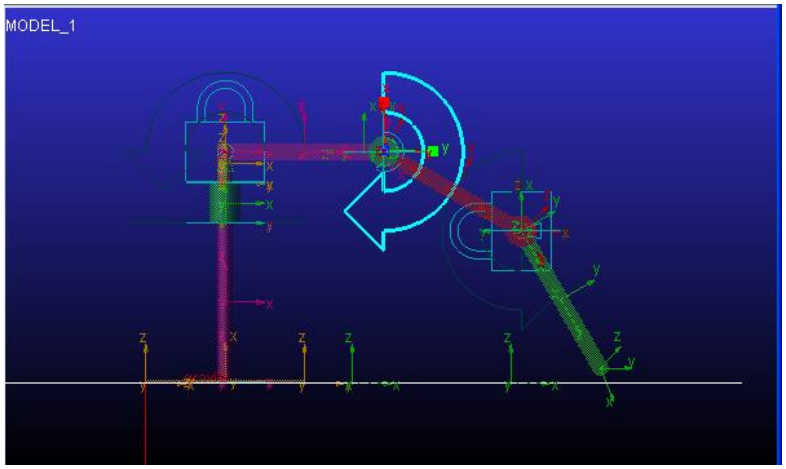

Figure8.1: Motion at joint 2

Now, the simulation is run for 3 sec (Stop time) with steps 50 and Torque curve were plotted in Graph tab by selecting the marker at that joint and selecting torque magnitude and torque vs. time curve was shown and also we measure the joint angle by using the angle measure from design exploration tab as explained above.

But we want to analyze the graph Torque vs. joint angle so we exported the values of torque from ADAMS to EXCEL and from there using graph tool we plotted the required graph for both cases with and without joint weight for clockwise and anti- clockwise rotation as shown below:

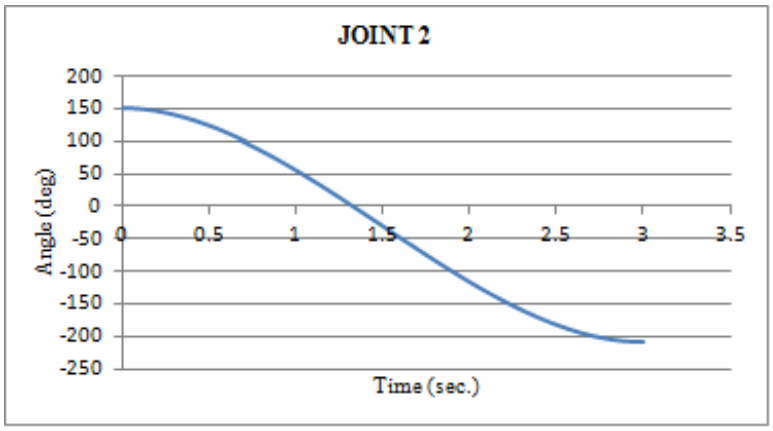

(a): Joint trajectory

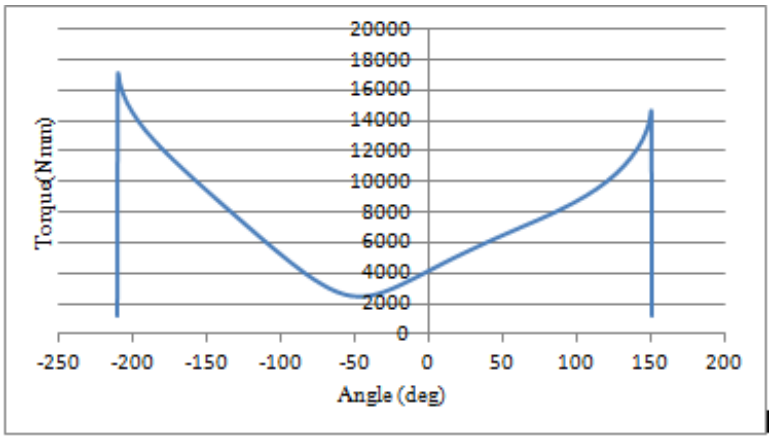

(b): Joint torque with weight attached

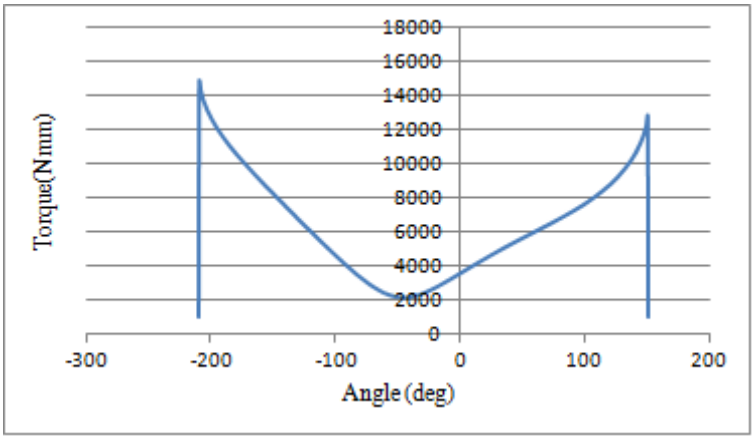

(c): Joint torque with no weight attached

Figure 8.2: Trajectory and torque of joint 2 in clockwise direction

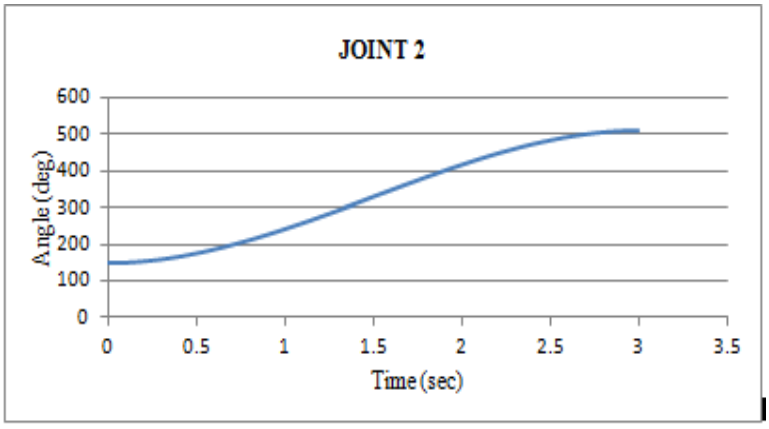

(a): Joint trajectory

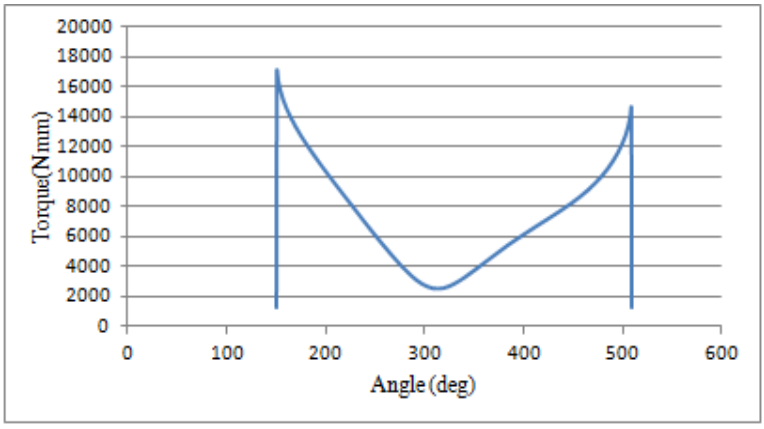

(b): Joint torque

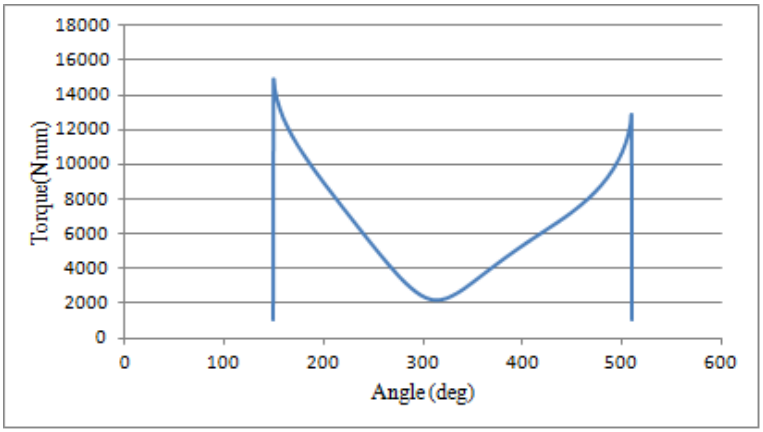

(c): Joint torque with no weight attached

Figure 8.3: Trajectory and torque of joint 2 in anti- clockwise direction

8.3.1 Comments

The first simulation task is to rotate joint 2 for 360 degrees in 0-3 sec time interval and the goal of this simulation is to analyze torque characteristics of joint with weight and without weight for both clockwise direction and anti clockwise rotation.

In order to move the robotic arm through this kind of trajectory, it is consequently found that the joint should follow the trajectories shown in Fig 8.2(a), 8.3(a) and from torque graphs we can see that initially magnitude of torque is greater in case of anti-clockwise rotation which is 17.1 Nm as seen in fig. 8.3(b) because it has to act in opposite direction to the inertial torque whereas in case of clockwise rotation, initial direction of torque due to motion and inertia are same so less torque is needed to move the robotic arm which is 14.63Nm as seen in fig. 8.2(b).

Also if we remove weight from the joint 2 then we can see magnitude of torque decreases to 14.9 Nm in case of anti- clockwise rotation as seen in fig. 8.3(c) which is obvious as less torque is required to lift the arm due to decrease in overall weight and same in case of motion in clockwise direction, value of torque decreases to 12.86 Nm as seen in fig. 8.2(c).

8.4 Rotation of joint 3:

Now, joint 3 is rotated clockwise and anti- clockwise while other joints are kept fixed by changing their feature from revolute joint to fixed joint as shown in fig .

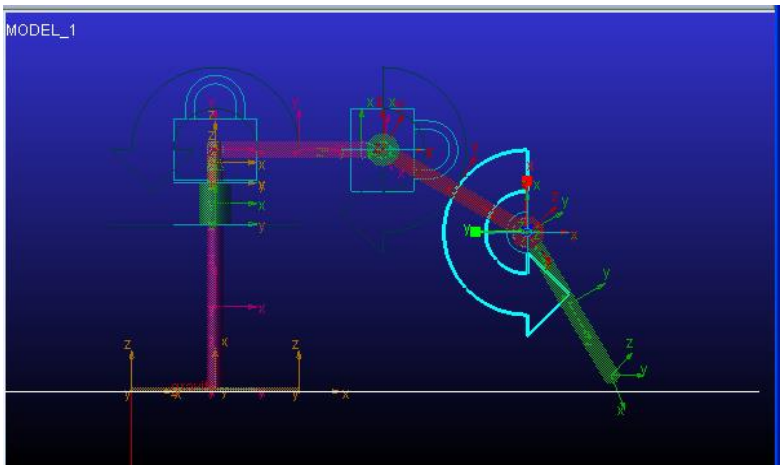

Figure 8.4: Motion at joint 3

Now, the simulation is run again for 3 sec (Stop time) with steps 50 and Torque curve were plotted in Graph tab by selecting the marker at that joint and selecting torque magnitude and torque vs. time curve was shown and also we measure the joint angle by using the angle measure from design exploration tab as explained above.

But we want to analyze the graph Torque vs. joint angle so we exported the values of torque from ADAMS to EXCEL and from there using graph tool we plotted the required graph for both clockwise and anti- clockwise rotation as shown below:

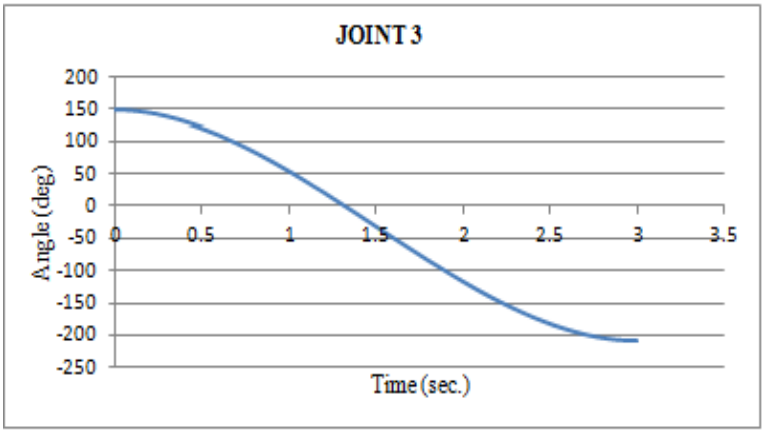

(a): Joint trajectory

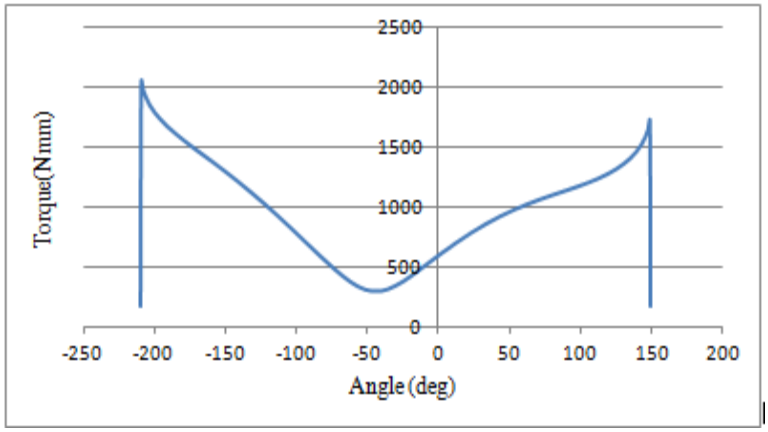

(b): Joint torque

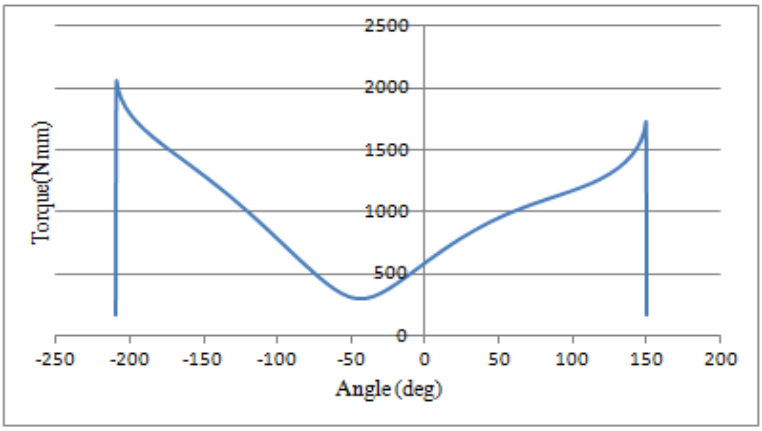

(c): Joint torque with no weight attached

Figure 8.5: Trajectory and torque of joint 3 in clockwise direction

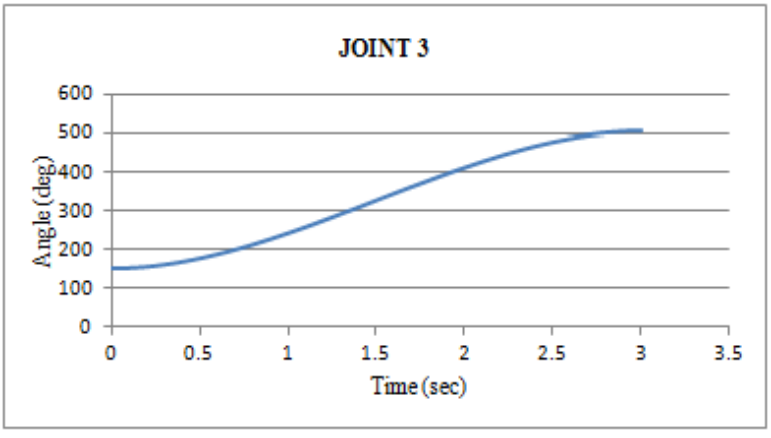

(a): Joint trajectory

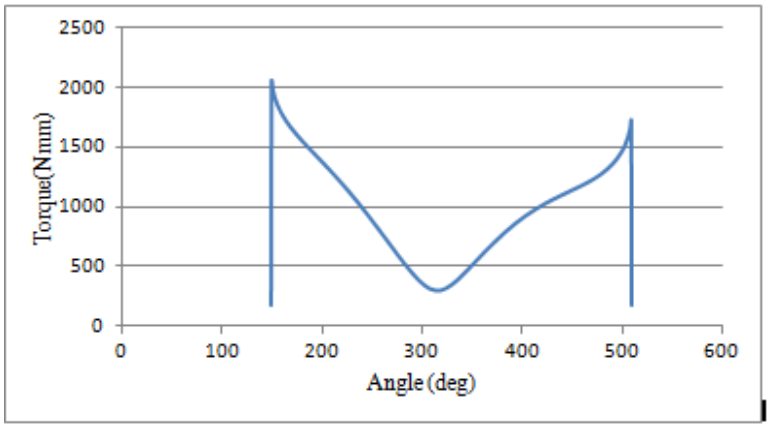

(b): Joint torque

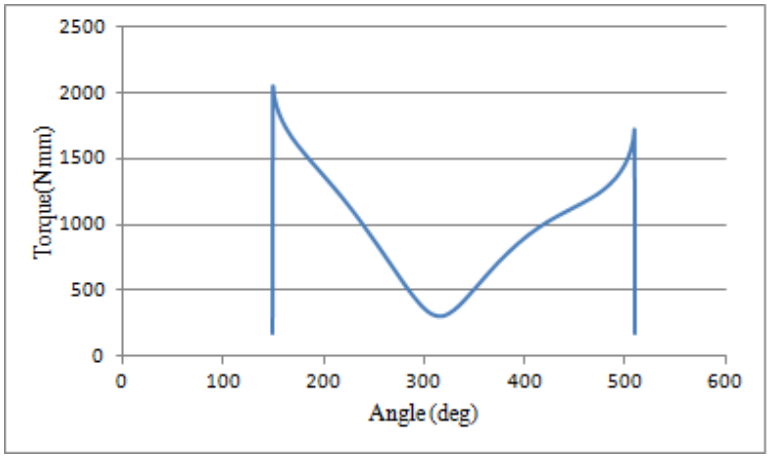

(c): Joint torque with no weight attached

Figure 8.6: Trajectory and torque of joint 3 in anti- clockwise direction

8.4.1 Comments

The second simulation task is to rotate joint 3 for again 360 degrees in 0-3 sec time interval and analyze the torque characteristics for this joint in both clockwise and anti- clockwise direction.

After performing the simulation we found that joint follow the same trajectory as in previous case shown in fig 8.3(a), 8.5(a) and torque graphs can be analyzed as explained in previous case i.e. in case of anti-clockwise motion value of torque is 2.055 Nm as seen in fig. 8.6(b) and in case of motion in clockwise direction, value of torque is 1.723 Nm as seen in fig. 8.5(b).

Now, again if we remove weight from the joint 3, we find that there is negligible change in value of torque i.e. 2.052Nm in case of anti-clockwise rotation as seen in fig. 8.6(c) because weight

acting at this joint is very small as compared to previous joint and same in case of rotation in clockwise direction, value of torque is 1.721 Nm as seen in fig. 8.5(c). Also we should note that in case of joint 3 value of torque decrease gradually as seen in previous case.

8.5 Movement of end effecter:

Now, as this robotic manipulator will be used for surgical purpose so the end effecter should move in a straight line so in this case we have removed constraints from every joint and motion is given to end effecter i.e. at the tip of link 3 using general point motion feature and is moved along the shown vertical(black) line.

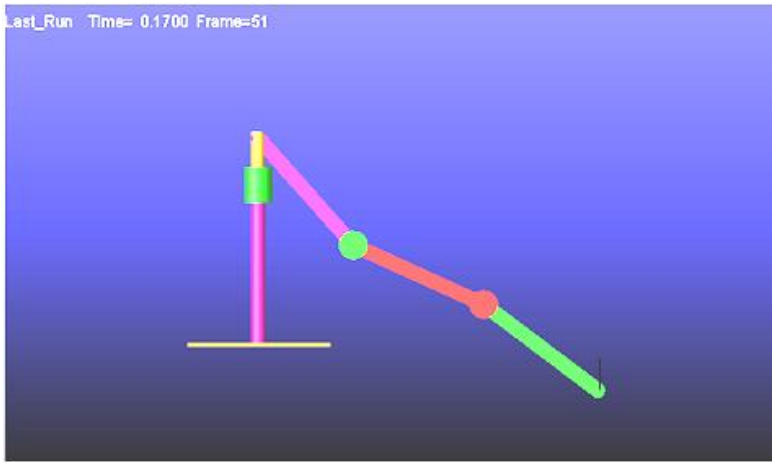

Figure 8.7: Motion at end effecter

So, simulations were run for 0.22 sec with steps 50 and torque at every joint is plotted as shown below:

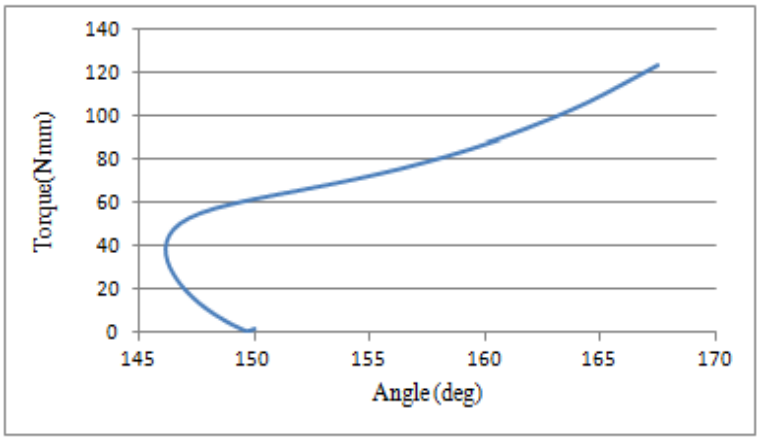

(a): Torque vs. Angle for joint 3

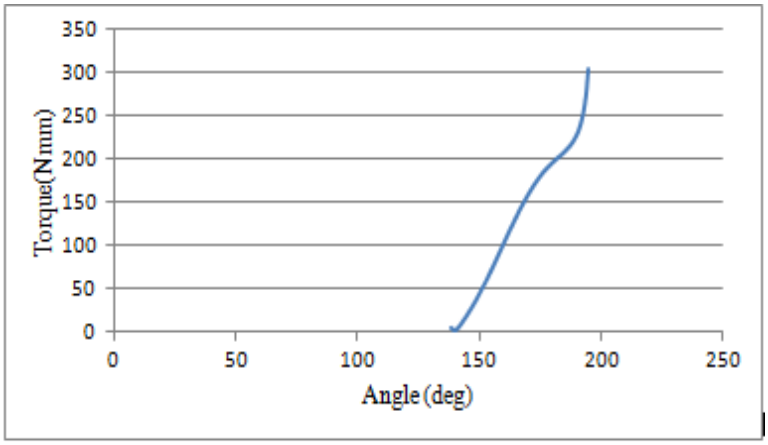

(b): Torque vs. Angle for joint 2

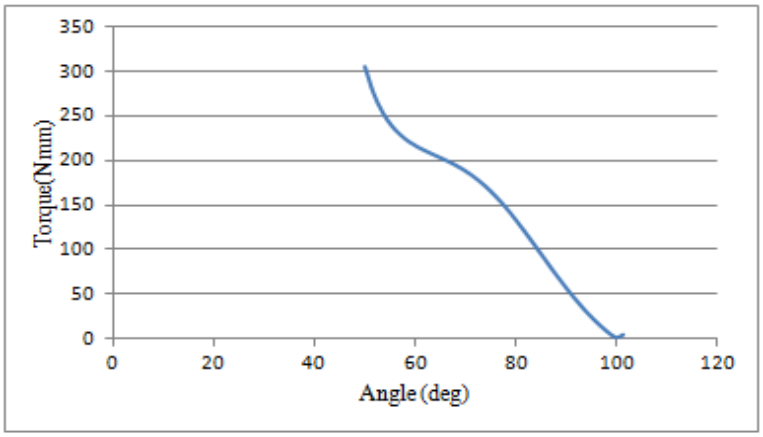

(c): Torque vs. Angle for joint 1

Figure8.8: Joint torque due to end effecter movement

8.5.1 Comments

The third simulation task is to move the end effecter in vertical direction and goal is to analyze the torque characteristics of each joint. For each joint torque increases with time and also in case of joint 1 and joint 2 there is no change in joint torque.

8.6 Rotation of joint with motor feature

We have applied steeper motor at both joint 2 and joint 3 but for analyzing the torque characteristics of each joint we have simulate the robotic manipulator with motor employed at one joint at a time.

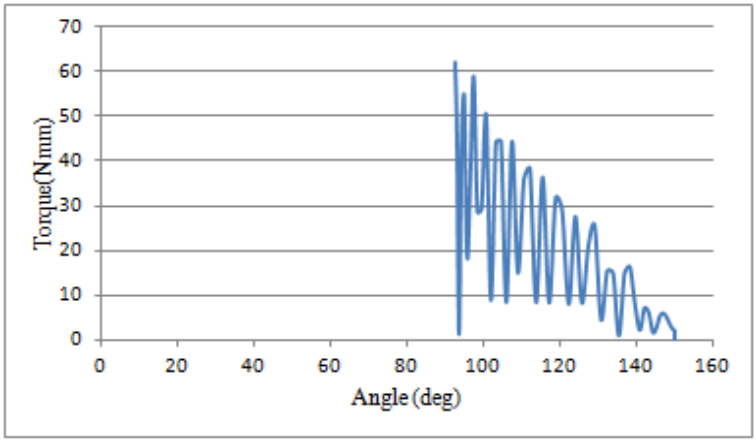

(a): Torque vs. Angle for joint 3

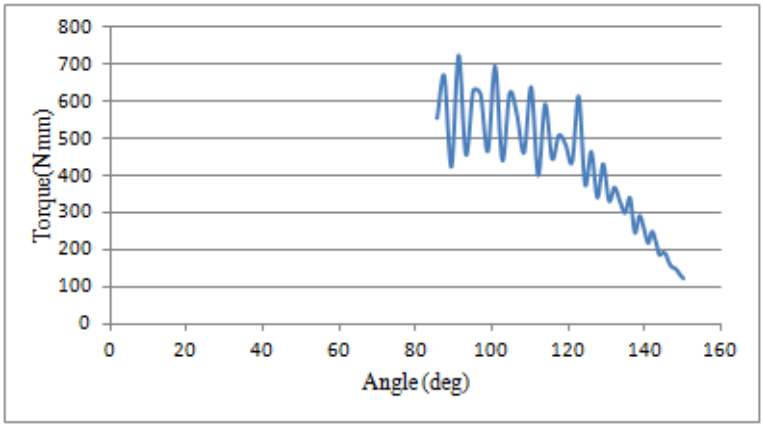

(b): Torque vs. Angle form joint 1

Figure 8.9: Joint torque with stepper motor

8.7 Trajectory of end effecter

As this project is specifically done for surgical purpose, we want to move our end effecter in specified direction i.e. in straight line and for that certain constraints are set which are explained in section 4.3. Now, we will apply the STEP function for our simulation purpose with expression

STEP (time, 0, 0, 0.5, 200)

i.e. the end effecter will move travel 200mm distance in z-axis in 0.5 sec time interval and we will use post processor for further analysis and discussion. Now, for analyzing the movement we have to first plot the end effecter movement i.e. Length vs. time plot. We can see from figure 8.10 that movement of end effecter is according to the input function. For the selection of appropriate motor and gear head we will analyze the torque characteristics of each joint. Now, from figure 8.11 we can see the torque variation for all three joints, we are getting maximum torque at around 145mm which are 608.11 Nmm ,608.11 Nmm and 865.23Nmm for joint 1, joint2 and joint 3 respectively. So, we can say that for joint 1 and joint 2 the variations of torque are same because the movement of joint 1 and joint2 are not that different for this specific interval and inertia of links are slightly different. We can also conclude that major change in the torque profile is in the 0.25-0.35 time interval and we have to select motor and gear head while keeping these things in mind as only these values will affect the capabilities of the motor and gear head.

Also for the analysis of the end effecter, it is important to consider the translational velocity and acceleration of the end effecter which is given in figure (8.12) and figure (8.13). We can easily say that for the operation of surgical tool, it must increase its velocity and then will decrease at the end of the interval and this is what happening in figure (8.12) and also in figure (8.13), abrupt profile is in the 0.3-0.4 time interval and after closely analysis, we can say that it is due to no mass attached at that point during simulation and ADMAS is not able to generate perfect profile and we can suppress this error later by attaching a point mass at that point.

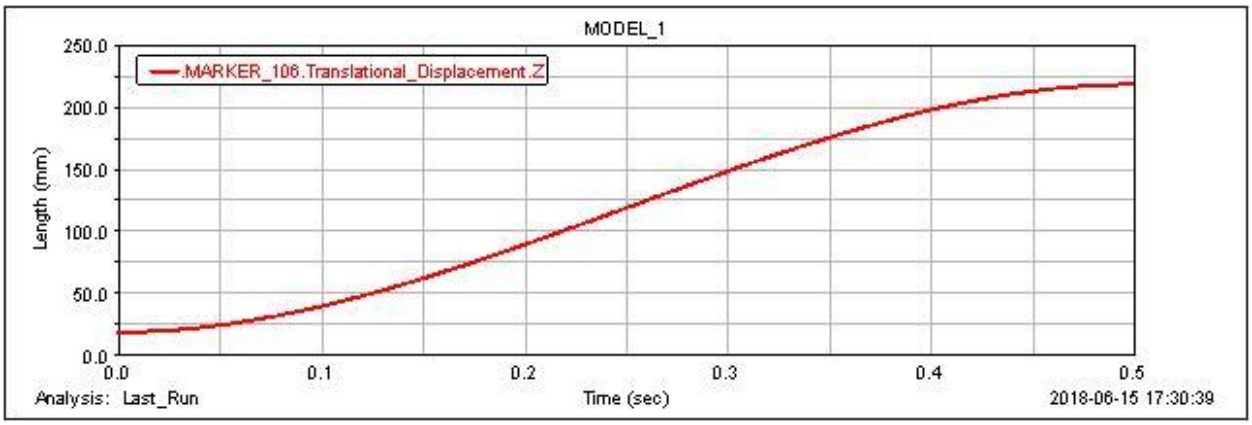

Figure 8.10: Movement of end effecter in z-axis

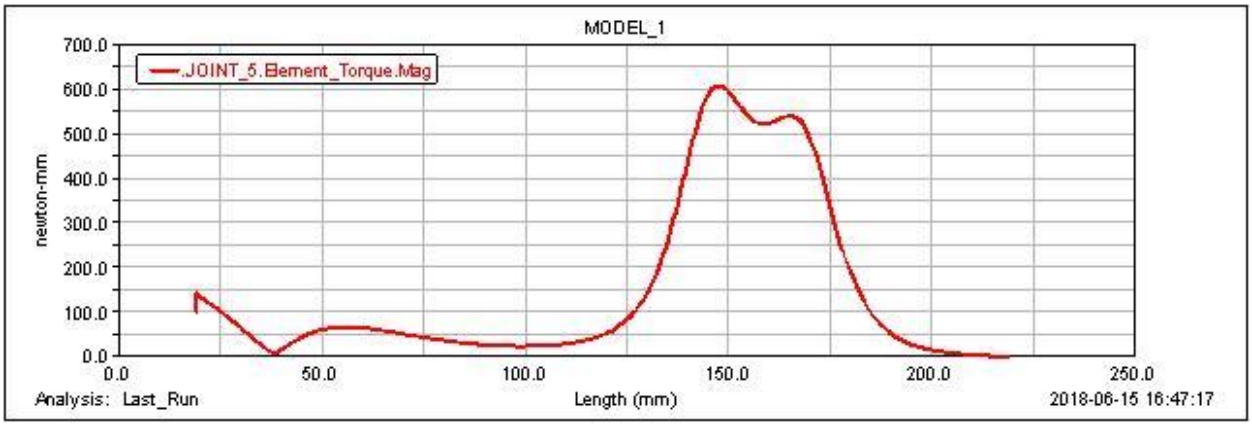

(a): Joint 1torque

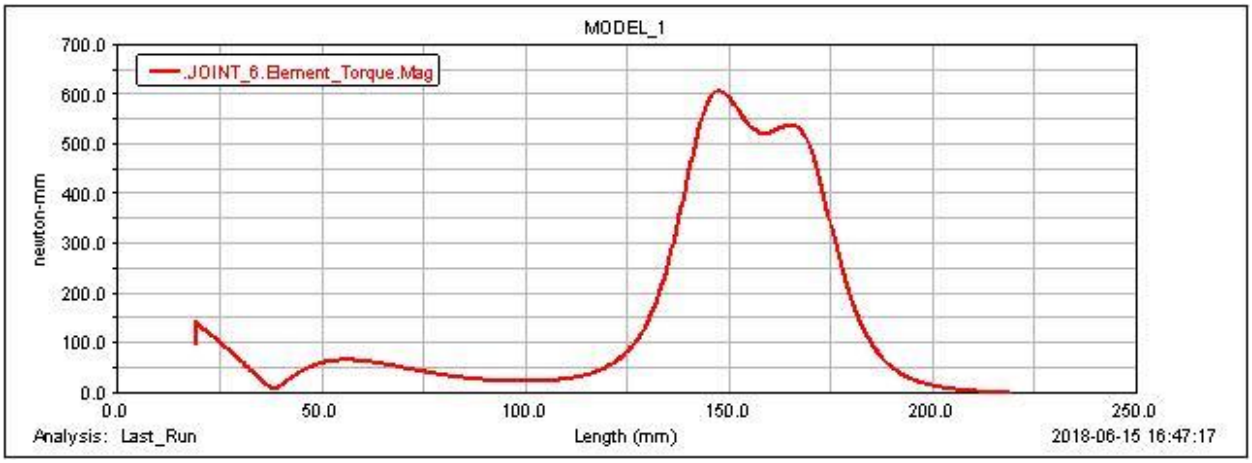

(b): Joint 2 torque

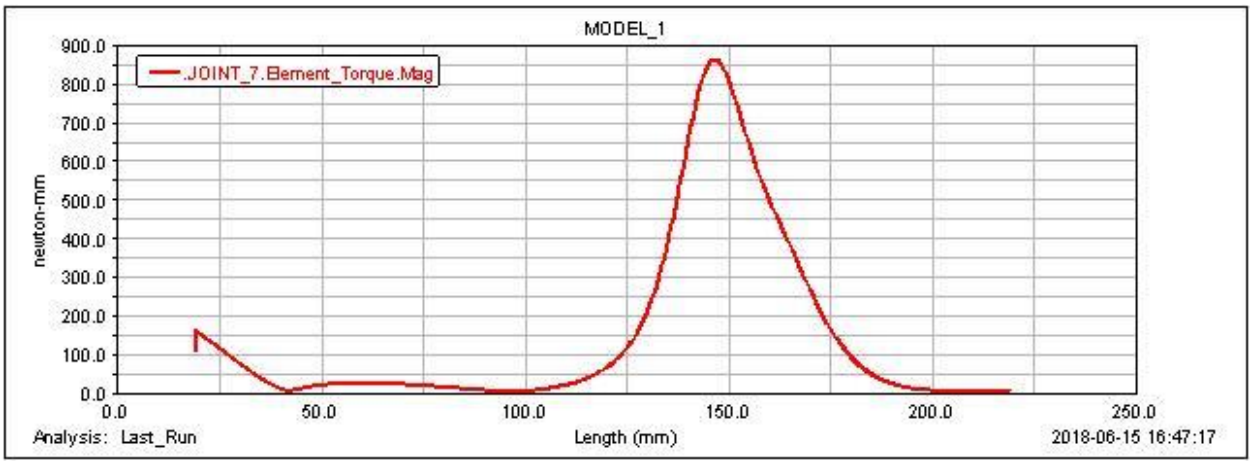

(c): Joint 3 torque

Figure 8.11: Joint torque trajectory

Figure 8.12: End effecter linear velocity

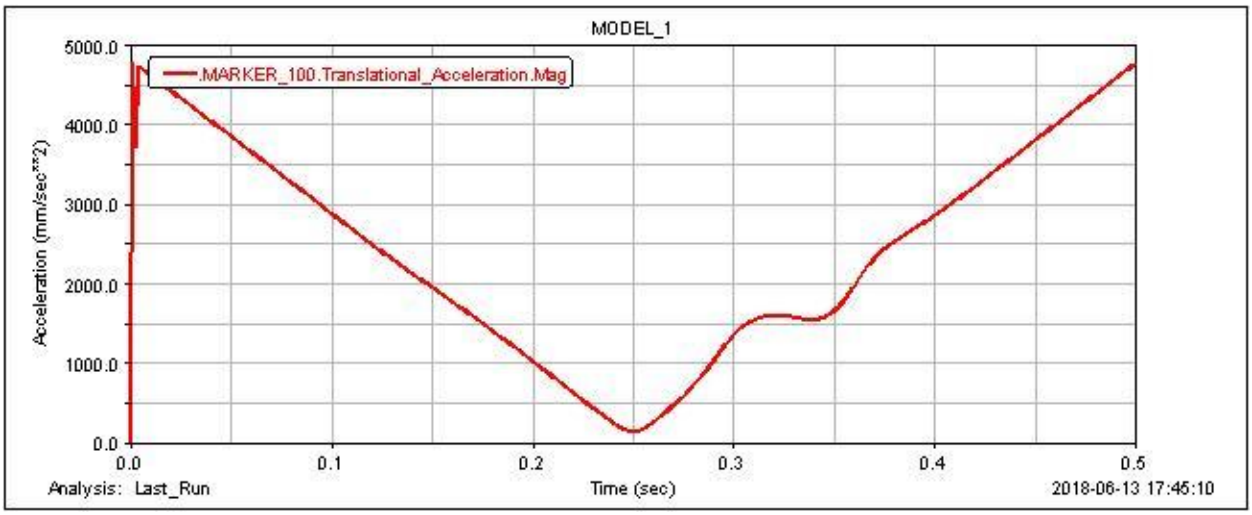

Figure 8.13: End effecter linear acceleration

8.7.1 Motor and gear head selection

Now, after collecting data and values for calculation of motor and gear head selection, we can apply formulas to get the required result.

We will be choosing the motor and gear head with the value from previous plots and using the equation from section 4.2.3 and section 4.3.2 and same applies for each joint and as we have seen that torque profile of joint 1 and joint 2 are same, the motor and gear head will be same for both the joints.

For Joint 3:

Index no.	Maxon motor	T_m (mNm)	T_m^{max} (mNm)	N_m^{max} (rpm)	Rotor inertia (gcm^2)	Mass (g)
1.	DCX 26L	57.8	695	9690	21.4	170

Index no	Ratio	Maxon Gearhead	T_g (Nm)	T_g^{max} (Nm)	N_g^{max} (rpm)	J_g (gcm^2)	Mass (g)
1.	16	GPX 26LN	1.8	2.25	8000	-	95

Table 8.1: Motor and gear head for joint 3

For joint 2:

Index no.	Maxon motor	T_m (mNm)	T_m^{max} (mNm)	N_m^{max} (rpm)	Rotor inertia (gcm^2)	Mass (g)
1.	DCX 19S	11.1	73.2	10600	2.75	50

Index no	Ratio	Maxon Gearhead	T_g (Nm)	T_g^{max} (Nm)	N_g^{max} (rpm)	J_g (gcm^2)	Mass (g)
1.	35	GPX 19HP	0.9	1.15	12500	-	51

Table 8.2: Motor and gear head for joint 2

For joint 1:

Index no.	Maxon motor	T_m (mNm)	T_m^{max} (mNm)	N_m^{max} (rpm)	Rotor inertia (gcm^2)	Mass (g)
1.	DCX 19S	11.1	73.2	10600	2.75	50

Index no	Ratio	Maxon Gearhead	T_g (Nm)	T_g^{max} (Nm)	N_g^{max} (rpm)	J_g (gcm^2)	Mass (g)
1.	35	GPX 19HP	0.9	1.15	12500	-	51

Table 8.3: Motor and gear head for joint 1

8.7.2 Comments

We have selected the required motors for the joint of the robotic manipulator and for building the realistic model; we need to mode these motors at joints by assuming the dead weights and specifying the same mass and density to the dead weights as shown in figure (8.14).

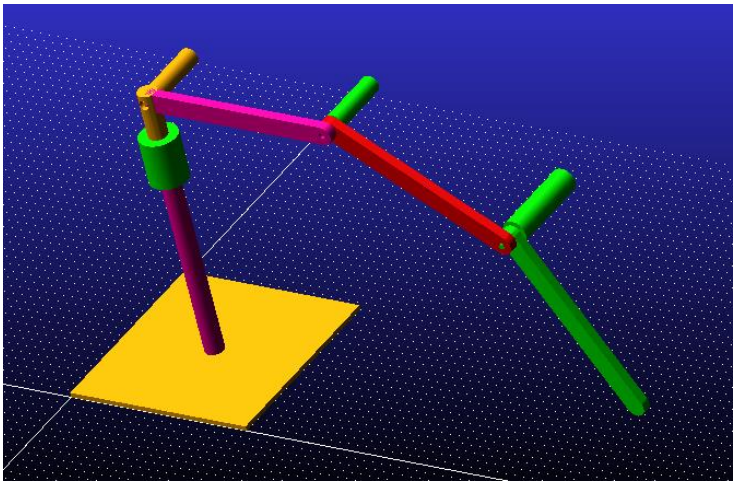

Figure 8.14: Motors attached to the manipulator

Location of motor	Length (mm)	Radius(mm)	Mass(kg)	Density(kg/mm^3)
Joint 1	65	9.5	0.1	5.36E-006
Joint 2	65	9.5	0.1	5.36E-006
Joint 3	87.2	13	0.26	5.61E-006

Table 8.4: Specifications of the motors

We will be plotting the same plots and will compare the results after attaching the motor to the joints. As we can see that maximum torque values are 2387.44 Nmm, 2973.63Nmm, 2998.79Nmm for joint 3 , joint2 and joint 1 respectively as shown in figure (8.15). These values occur when both links becomes straight at around 0.426 sec. Same problem still persists for end effecter linear acceleration as shown in figure (8.16) because still we haven't attached a point mass at the end effecter.

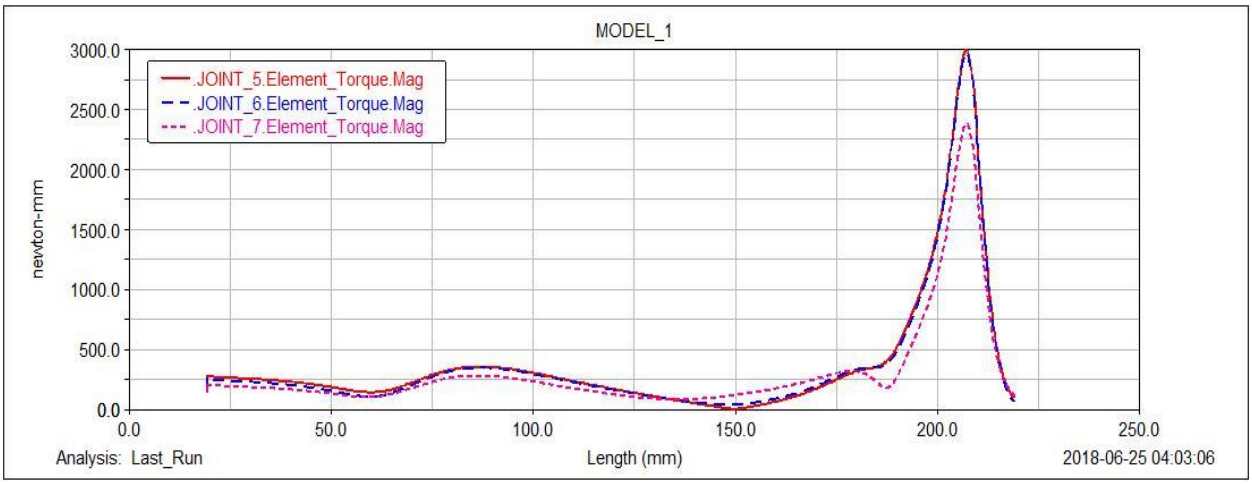

Figure 8.15: Joint torques trajectory

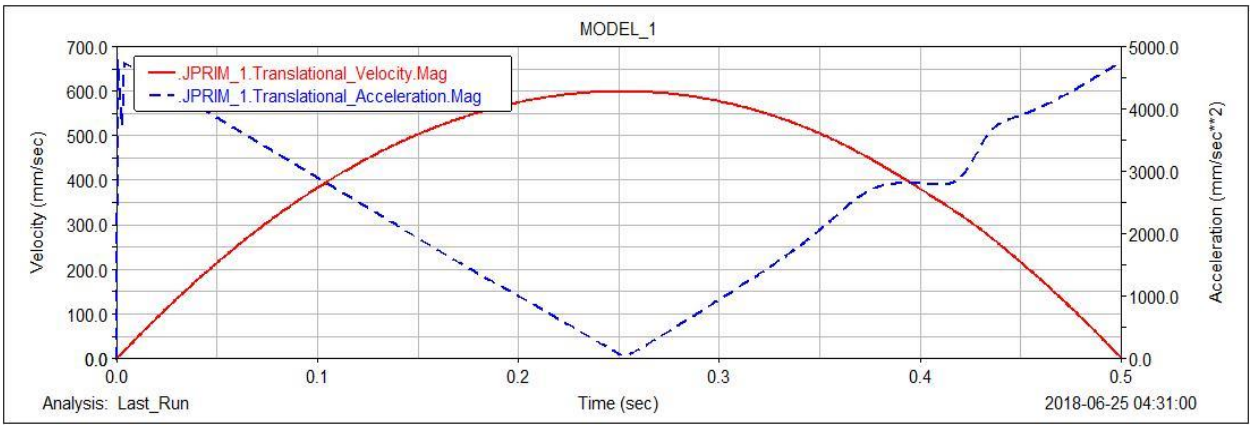

Figure 8.16: Linear velocity and acceleration of end effecter

Now, we will be adding friction value which we have calculated previously and also a point mass for more realistic model and as the application will be related to surgery, so we are adding 400gm mass only for seeing the changes in the generated plots.

In figure 8.17, where pink line represents joint 3 torque, blue line represents joint 2 torque and red line represents joint 1 torque, we can see that value of torques has increased by addition of extra weight and friction at the joints of the manipulator. Values are 2745.9Nmm, 3421.03 Nmm and 3446.27 Nmm for joint 3, joint 2 and joint 1 respectively. As point mass is added at the end effecter, so more torque will be experienced at the maximum distance i.e. joint 1 will experience more torque than joint 2 and joint 1 and that's why we getting the highest value for the joint 1 and similarly we can concluded for the other joints. Also, these maximum values again occur when the links are straight at 0.424 sec.

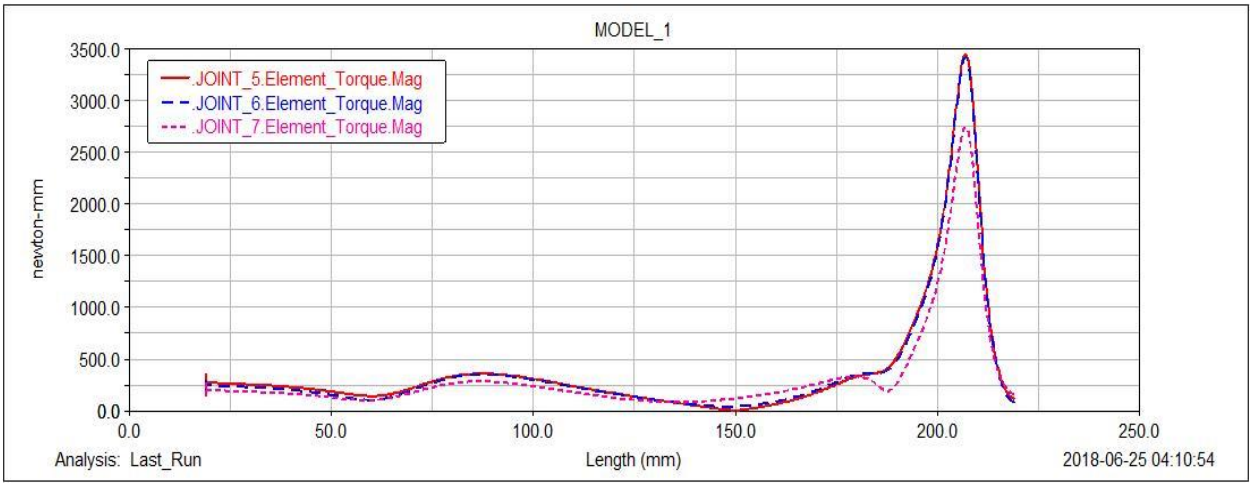

Figure8.17: Joint torques trajectory

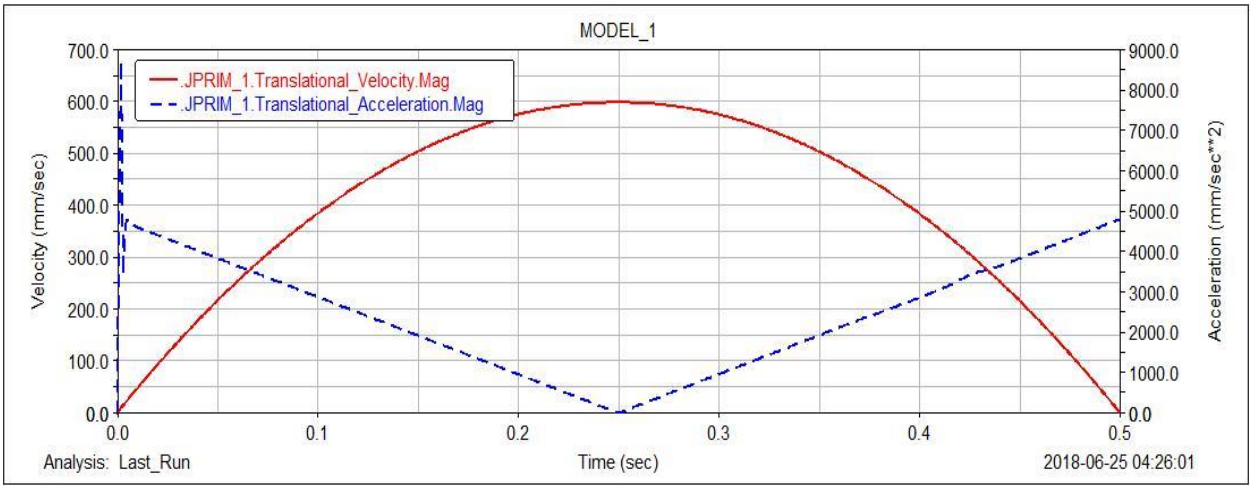

Figure 8.18: Linear velocity and acceleration of end effecter

Chapter 9

Conclusions

This chapter presents a concluding summary of the project, as well as recommendations for improvement and further work.

9.1 Summary

The topic of this project has been dynamic analysis of robotic manipulator. Modeling of the robotic manipulator was performed in ADAMS platform and thus introduced the main parameters used to model the system with greater accuracy. Various friction models are available for estimating the friction in joints but we have used the model specific to our purpose. Constraints were formulated by considering both motor and gearbox characteristics and robot arm dynamics.

It has been shown that estimating the right torque characteristics is a time consuming challenge. So, modeling of the manipulator and analyzing the torque pattern and then considering the values required for selecting and sizing the motor and gearbox specific to each and every joint of the manipulator was very important. In this model, the properties have been estimated based on inspecting the manipulator trajectory very carefully and this is achieved by stopping simulations at every crucial time frame and analyzing the joint angle variation and how the links of the manipulator are behaving.

Simulations of the manipulator are important and have a main purpose in proving the validity of the model. Simulation without considering the attached motor and expected friction between the joints is of no importance and thus we have to work on both things simultaneously and at the end we need to combine these tasks to give realistic behavior to the model.

Also, while analyzing the dynamics of the manipulator, there is a need to think of the parameters which best describes the behavior of the model like the use of linear velocity and linear acceleration plots of the end effecter, these plots are crucial to identify the importance of mass at the end effecter and for that point mass was attached to the end effecter for plotting the correct torque pattern.

9.2 Contributions

- Complete model of RRR robotic manipulator, including simulations that demonstrates the behavior of required trajectory.
- Detailed description of friction model used for the incorporation of joint friction.
- Underlying theory of the motor selection and sizing and how to incorporate and implement in ADMAS model for simulation purpose.

9.3 Recommendations for Future Work

We have modeled the manipulator through the use of software and for validation it is important but there is need to generate code to perform several iterations easily and for that derivation of dynamic model is given in the report which can help to generate the algorithm and can be implemented in any platform like MATALB. The dynamic parameters in this thesis are estimated roughly, and there is much potential for improvement in this project.

The optimization done in this project is focused mainly on the mechatronic part of the robotic arm. Crucial component of system design is robot control part and is a key competence for robot manufacturers and important for getting more performance or efficiency out of a robot. Tuning of control parameters is also crucial for a robotic arm. So most important work can be to combine both part i.e. mechanical design and control design in the whole system optimization.

Also there are certain limited aspects in this model. A perfect model will include joint flexibility also and there would be bounds on the maximum input torque for the motors. Also Inverse dynamics control can be included in future work for trajectory tracking of the manipulator. Trajectory tracking is required to avoid collisions with obstacles within the workspace of the manipulator.

Chapter 10

Bibliography

[1]. http://www.csio.res.in/CommonNew.php?ds=69&page=1.

[2]. http://www.csir.res.in/about-us/vision-and-mission

[3]. http://www.csio.res.in/CommonNew.php?ds=68&page=1

[4]. https://en.wikipedia.org/wiki/Central_Scientific_Instruments_Organisation

[5]. http://www.csio.res.in/CommonNew.php?ds=108&page=1

[6]. Briot S. and Bonev I.A., "Are parallel robots more accurate than serial robots?" CSME Transactions Vol 31, No 4, 445-456, 2007.

[7]. http://www.gametechinternational.com/gti_index/l5ace-kt-750.jpg

[8]. http://www.superdroidrobots.com/images/customPages/HD2-Gen5-5Axis.jpg)

[9]. ABB Robotics. Product specification for IRB 140, Retrieved September 21, 2010

[10]. http://www.strongarmindustries.com/images/strongarm/electric1.jpg

[11]. http://www.3mech.titech.ac.jp/ms_sugimoto/ms_sugimoto_images/hybrid_parallel.JPG

[12]. MSC Software. 2005. MSC.ADAMS® MSC. Software Corporation, Santa Ana, CA. http://www.mscsoftware.com/

[13]. M.W. Spong, S. Hutchinson, and M. Vidyasagar. Robot modeling and control. Wiley New Jersey, 2006.

[14]. Armstrong-Hélouvry et al., 1994.

[15]. Adaptive friction compensation with dynamic friction model C. Canudas-de-Wit and P. Lischinsky', 1996.

[16]. Adaptive friction compensation with dynamic friction model C. Canudas-de-Wit and P. Lischinsky', 1996

[17]. MSC. Software Corporation, "MD Adams R3 Help Documentation", 2008.

[18]. "Friction modeling and parameter estimation for hydraulic cylinders"- Master thesis, 2011

[19]. B. Siciliano, L. Sciavicco, L. Villani, and G. Oriolo, Robotics: modeling, planning and control. Springer Science & Business Media, 2009

[20]. B. Siciliano, L. Sciavicco, L. Villani, and G. Oriolo, Robotics: modeling, planning and control. Springer Science & Business Media, 2009

[21]. Fieback, M. C. R., R. M. Van Schelven, and M. A. Seuters. "A Robotic Arm for Zebro." (2015).]

[22]. https://www.maxonmotor.in/medias/sys_master/root/8804420648990/gear-Das-wichtigste-ueber-getriebe-11-DE-EN-ES-030-031.pdf?attachment=true

[23]. Craig, John J. *Introduction to robotics: mechanics and control*. Vol. 3. Upper Saddle River, NJ, USA:: Pearson/Prentice Hall, 2005.

[24]. Mike Blundell and Damian Harty. Multibody Systems Approach to Vehicle Dynamics.SAE International, 2004. ISBN 0768014964.

[25]. MSC Software Corporation. Adams help. Electronic, 2013.2.